Master Project

# Geometrically Exact 2D Beam Theories: Finite Element Formulations and Comparative Analysis

Vahab Narouie

Nonlinear theories for beams were developed in the last three decades. They all can be applied for finite element discretization. This paper is based on the formulation of nonlinear rod and beam theories, which have, as the only restriction, the classical assumption of "plane cross sections remain plane." No other approximations are made; hence, the strains, deflections, and rotations can be finite, and these theories are called geometrically exact. The development of these beam theories goes back to the work by Reissner (1972). A generalization for the three-dimensional case can be found in Simo (1985). Based on this theoretical background, several authors developed associated finite element formulations. Therefore, different beam theories are considered for the two-dimensional case. Additionally, associated numerical formulations are derived for finite element implementations. The theories are then compared by means of examples which depict the limits in the application of different approaches.

1. edition: May 9, 2017
2. edition: January 6, 2024

Institute of Mechanics and Dynamics
Prof. Dr.-Ing. habil. Detlef Kuhl
University of Kassel
Department of Civil and Environmental Engineering
Mönchebergstraße 7
34109 Kassel, Germany
www.uni-kassel.de/fb14/mechanics

# Contents

# List of Figures

# List of Tables

# Chapter 1

# Introduction

Nonlinear theories for beams have been developed over the past three decades. All of them apply to finite element discretization. Generally, three distinct approaches must be identified.

1. The first approach is based on the assumption of small strains. It involves a frame undergoing finite rigid rotations and formulates strains and stresses relative to its rotations, known as the co-rotational formulation. This approach requires the strains to be small but allows for investigating large deflections and rotations. Finite element schemes based on such formulations can be found in works such as Oran and Kassimali (1976), Wempner (1969), Rankin and Brogan (1984), Lumpe (1982), Crisfield (1991), and Crisfield (1997).

2. The second approach utilizes continuum equations and incorporates beam kinematics through specific isoparametric finite element interpolations. Known as the degenerated continuum approach, examples of this method can be found in Bathe and Bolourchi (1979), Dvorkin et al. (1988), and the textbooks by Bathe (1996) and Crisfield (1997).

3. The third approach is grounded in the formulation of nonlinear rod and beam theories, which adhere solely to the classical assumption that "plane cross sections remain plane." This approach makes no further approximations; thus, strains, deflections, and rotations can be finite. These theories are referred to as **geometrically exact**. The development of these beam theories dates back to the work of Reissner (1972). A generalization for the three-dimensional case is presented in Simo (1985). Building on this theoretical foundation, several authors have developed associated finite element formulations, as seen in Simo and Vu-Quoc (1986), Pimenta and Yojo (1993), Jelenic and Saje (1995), Gruttmann et al. (1998), and Mäkinen (2007). For a nonlinear formulation of curved beam elements, refer to Ibrahimbegovic (1995). Gruttmann et al. (2000) considered elasto-plastic material, and Romero and Armero (2002) incorporated dynamics within the geometrically exact framework.

The latter beam theories also encompass the arbitrary loading of truss and cable structures, thus allowing for general application to one-dimensional construction elements. However, apart from very limited and simplified examples, these nonlinear beam theories cannot be solved analytically. Applying nonlinear beam formulations in the *finite element methods* (FEM) framework poses no difficulty. Consequently, many complex engineering problems can be resolved, such as a rotor blade or deploying an antenna structure in space.

However, even now, many software tools for civil engineering still use the so-called second-order theories as the basis for finite element implementation. These theories include nonlinear effects but are restricted to small rotations. They can be applied for limit load computations and stability investigations. These theories stem from the times when analytic solutions were needed to solve such problems; however, when using modern computers, the geometrically exact theories can be applied instead.

In this contribution, different beam theories are considered for the two-dimensional case. Additionally, associated numerical formulations are derived for finite element implementations. The theories are compared using examples that depict the limits of applying different approaches.

## 1.1 Beam Model

### 1.1.1 Basic Concepts and Terminology

Beams represent the most common structural component found in civil and mechanical structures. Because of their ubiquity, they are extensively studied analytically in Mechanics of Materials courses. Such a piece of basic knowledge is assumed here. The following material recapitulates the definitions and concepts needed in the finite element formulation.

A beam is a rod-like structural member that can resist transverse loading applied between its supports. By "rod-like," it means that one of the dimensions is considerably larger than the other two. This is called the longitudinal dimension and defines the longitudinal or axial direction. Directions normal to the longitudinal direction are called transverse. The intersection of planes normal to the longitudinal direction with the beam are called cross sections, just as for bar elements. The beam's longitudinal axis is directed along the longitudinal direction and passes through the centroid of the cross sections.

Beams can function as standalone structures or be combined to create framework structures, the latter being the most prevalent in high-rise building construction. Individual beam components within a framework are called members and are connected at joints. Frameworks differ from trusses because their joints are rigid enough to transmit bending moments between members.

In practical structures, beam members can take up various loads, including bi-axial bending, bidirectional shears, axial forces, and torsion. Such complicated actions are typical of spatial beams, used in three-dimensional frameworks and subject to forces applied along arbitrary directions. A plane beam resists primarily loading applied in one plane and has a cross-section with respect to that plane. Plane frameworks, such as the one illustrated in Figure 1.1, are symmetric assemblies of plane beams that share that symmetry. Those structures can be analyzed with two-dimensional idealizations. A beam is straight if the longitudinal direction is a straight line. A beam is prismatic if its cross-section is uniform. Only straight, prismatic, plane beams will be considered in this paper.

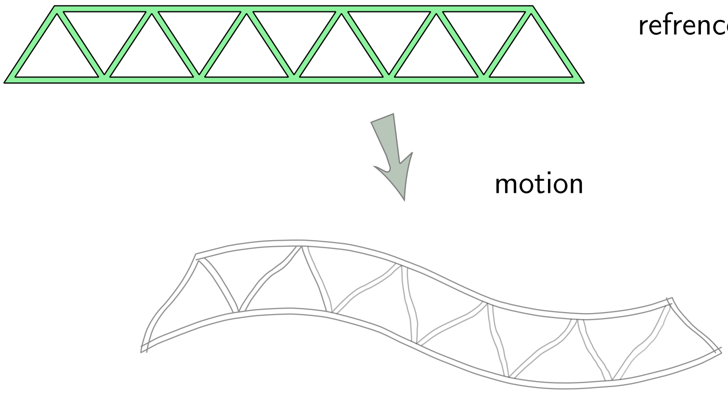


*Figure 1.1: A geometrically 2D nonlinear plane framework structure.*

### 1.1.2 Beam Mathematical Models

Beams are three-dimensional solids. One-dimensional mathematical models of plane beams are constructed based on beam theories. All such theories involve some form of approximation that describes the behavior of the cross sections in terms of quantities evaluated on the longitudinal axis. More precisely, the element kinematics of a plane beam is completely defined by the two models described below if the following functions are given:

- Axial displacement $u(X_1)$
- Transverse displacement $w(X_1)$ (also called lateral displacement)
- Cross section rotation $\psi(X_1)$ : angle by which cross section rotates.

Here, $X_1$ denotes the longitudinal coordinate in the reference configuration. See Figure 1.2.

There are two beam mathematical models commonly used in structural mechanics:

- Euler-Bernoulli Model: This model is also called classical beam theory or engineering beam theory and is covered in elementary treatments of Mechanics of Materials. It accounts for the bending moment's effects on stresses and deformations. Transverse shear forces are recovered from equilibrium, but their impact on beam deformations is ignored (more precisely, the strain energy due to shear stresses is neglected). The fundamental kinematic assumption is that cross sections remain plane and normal to the deformed longitudinal axis. This rotation occurs about a neutral axis parallel to $X_3$ that passes through the centroid of the cross-section.
- Timoshenko Model: This model corrects the Euler-Bernoulli theory with first-order shear deformation effects. The critical assumption is that cross sections remain plane and rotate about the same neutral axis but do not remain normal to the deformed longitudinal axis. The deviation from normality is produced by a transverse shear stress assumed to be constant over the cross-section.

Both the Euler-Bernoulli and Timoshenko models rest on the assumptions of small deformations and linear elastic isotropic material behavior. In addition, both models neglect any change

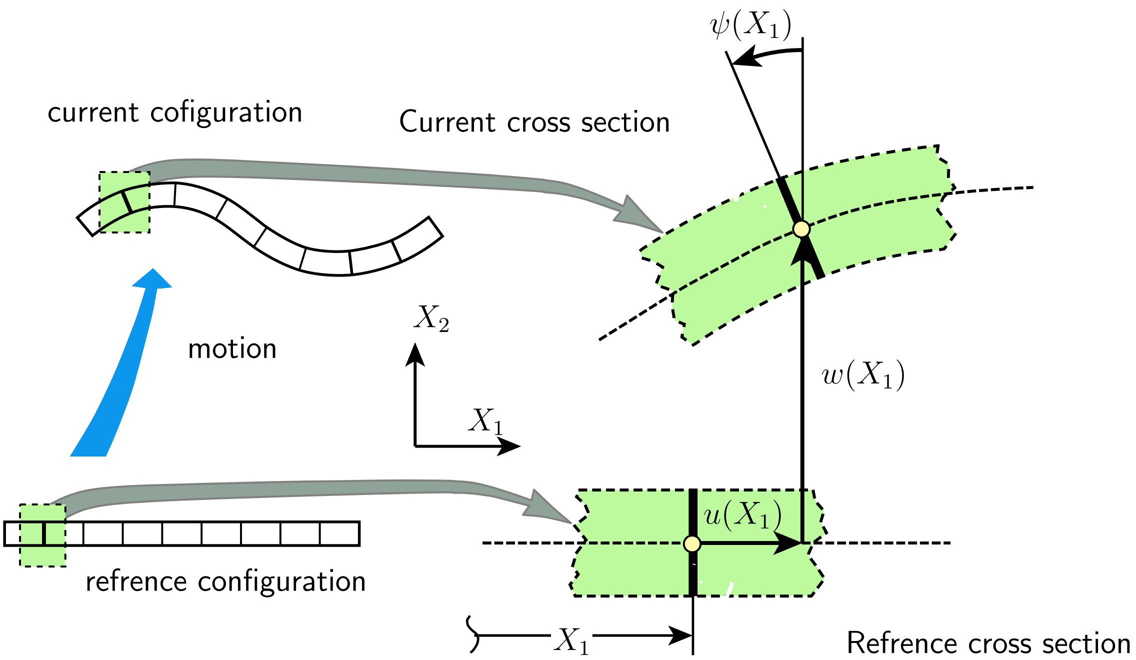


*Figure 1.2: Definition of beam kinematics in terms of the three displacement functions:* $u(X_1)$*,* $w(X_1)$ *and* $\psi(X_1)$*. The figure depicts the Euler-Bernoulli model of kinematics. In the Timoshenko model,* $\psi(X_1)$ *is not constrained by normality.*

in the dimensions of the cross sections as the beam deforms. Either theory can account for geometrically exact nonlinear behavior due to large displacements and rotations as long as the other assumptions hold.

### 1.1.3 Finite Element Models

To carry out the geometrically nonlinear finite element analysis of a framework structure, beam members are idealized as an assembly of finite elements, as illustrated in Figure 1.3. Beam elements used in practice usually have two end nodes. The $I^{th}$ node has three DOF: two-node displacements $u_I$ and $w_I$, and one nodal rotation $\psi_I$, positive counterclockwise in radians, about the $X_3$ axis. See Figure 1.4.

The cross-section rotation from the reference to the current configuration is called $\psi$ in both models. In the Eulerr-Bernoulli model, this is the same as the rotation $\phi$ of the longitudinal axis. In the Timoshenko model, the shear distortion angle is $\mu = \psi - \theta$, as shown in Figure 1.5. The mean shear strain has the opposite sign: $\bar{\mu} = \mu = \theta - \psi$, to make the shear strain $E_{11}$ positive, as per the usual conventions of structural mechanics.

Either the Euler-Bernoulli or the Timoshenko model may be used as the basis for the TL beam element formulation. Although the Timoshenko beam model appears to be more complex because of the inclusion of shear deformation, finite elements based on this model are simpler to construct. Here are the two key reasons:

- Separate kinematic assumptions on the variation of cross-section rotations are possible, as made evident by Figure 1.5. Mathematically: $\psi(X_1)$ may be assumed independently of $u(X_1)$ and $w(X_1)$. As a consequence, two-node Timoshenko elements may use lin-

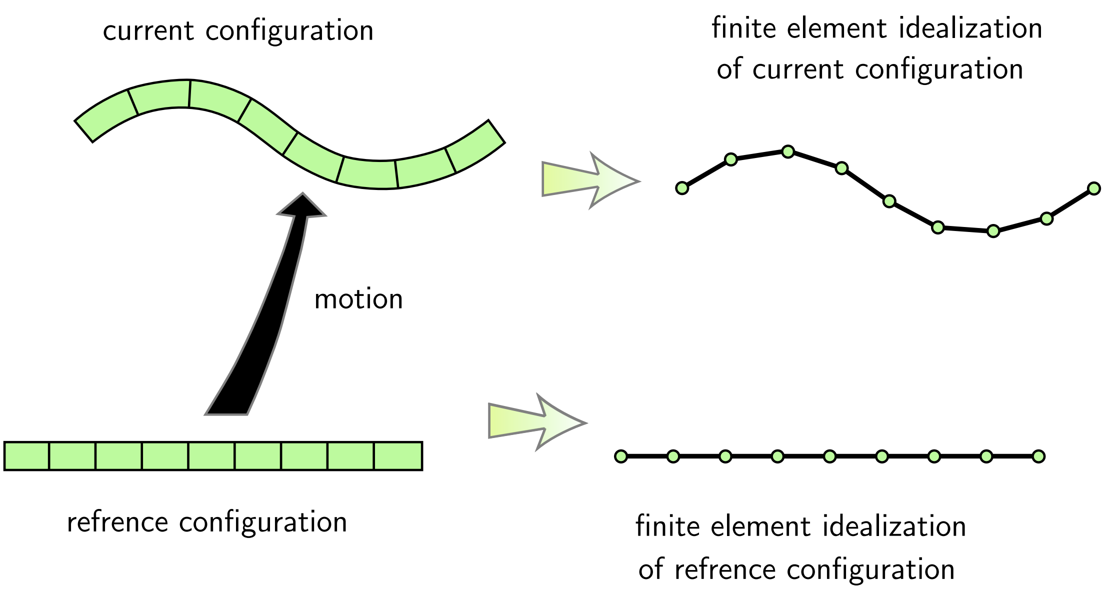


*Figure 1.3: Idealization of a geometrically nonlinear beam member as an assembly of finite elements*

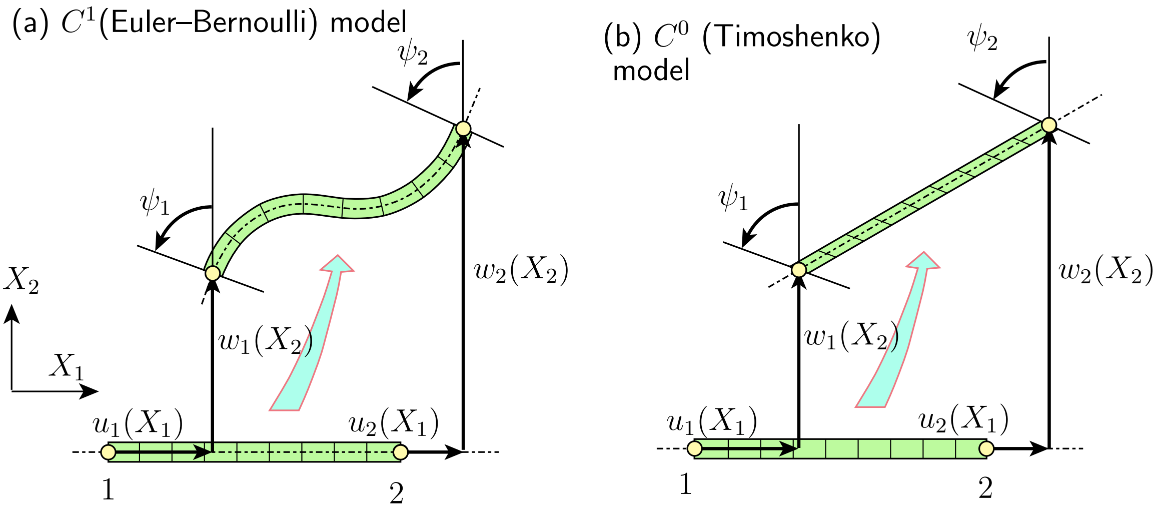


*Figure 1.4: Two-node beam elements have six DOF, regardless of the model used.*

ear variations in both displacement and rotations. On the other hand, a two-node Euler–Bernoulli model requires a cubic polynomial for $w(X_1)$ because the rotation $\psi(X_1)$ is not independent.

- The linear transverse displacement variation matches that commonly assumed for the axial deformation (bar-like behavior). The transverse and axial displacement assumptions are then said to be consistent.

### 1.1.4 Shear Locking

In the FEM literature, an Euler-Bernoulli-based model such as the one shown in Figure 1.4(a) is called a $C^1$ beam because this is the kind of mathematical continuity achieved in the longitudinal direction when a beam member is divided into several elements (See Figure 1.3).

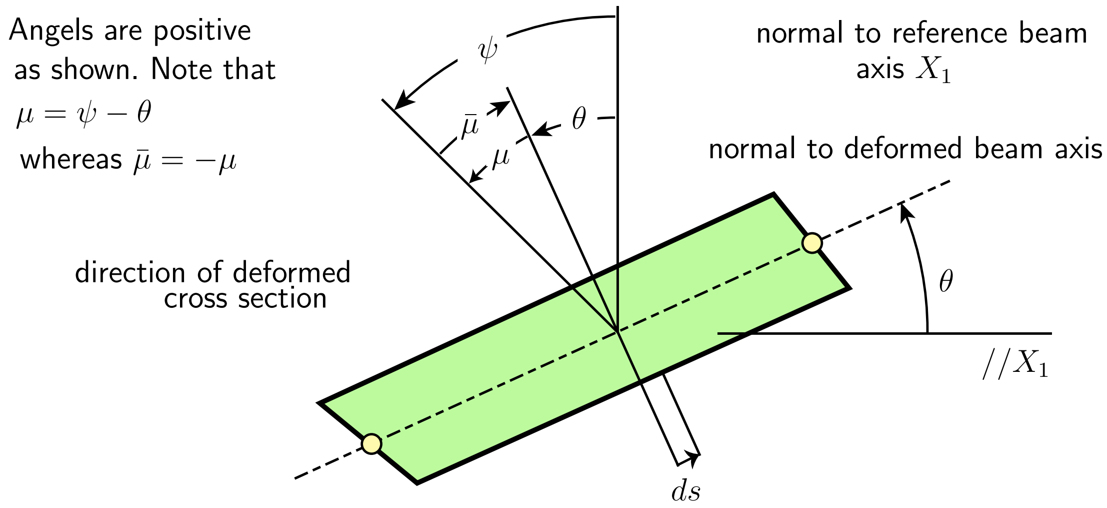


*Figure 1.5: Illustrates total and Euler–Bernoulli section rotations $\psi$ and $\theta$, respectively, in the plane beam Timoshenko model. The mean shear distortion angle is $\mu = \psi - \theta$, but we take $\bar{\mu} = -\mu = \theta - \psi$ as a shear strain measure to match the usual sign conventions of structural mechanics. For elastic deformations of engineering materials $|\bar{\mu}| << 1$. Typical values for $|\bar{\mu}|$ would be $O(10^{-3})$ radians, whereas rotations $\theta$ and $\psi$ may be much larger, say 1-2 radians. The magnitude of $\bar{\mu}$ is grossly exaggerated in the Figure for visualization convenience.*

On the other hand, the Timoshenko-based element pictured in Figure 1.4(b) is called a $C^0$ beam because both transverse displacements, as well as the rotation angle $\psi$, preserve only $C^0$ continuity.

What would be the first reaction of an experienced but old-fashioned (i.e, “never heard about FEM”) structural engineer on looking at Figure (1.6)?. The engineer would pronounce the $C^0$ element unsuitable for practical use. And indeed, the kinematics look way wrong. The shear distortion grossly violates the basic assumptions of beam behavior. And indeed, a huge amount of shear energy would be required to keep the element straight as pictured.

The engineer would be both right and wrong. If the two-node element of Figure (1.6)(b) were constructed with actual shear properties and exact integration, an over-stiff model results. This phenomenon is well known in the FEM literature and receives the name of shear locking. To avoid locking while retaining the element simplicity, it is necessary to use specific computational devices that have nothing to do with physics. The most common device is "Selective integration for the shear energy."

## 1.2 $X_1$-Aligned Refrence Configuration

### 1.2.1 Element Description

We consider a two-node, straight, prismatic $C^0$ plane beam element moving in the $(X_1, X_2)$ plane, as depicted in Figure 1.7. For simplicity, in the following derivation, the $X_1$ axis system is initially aligned with the longitudinal direction in the reference configuration. The reference element length is $L_0$. The cross section area $A_0$ and second moment of inertia $I_0$ are defined

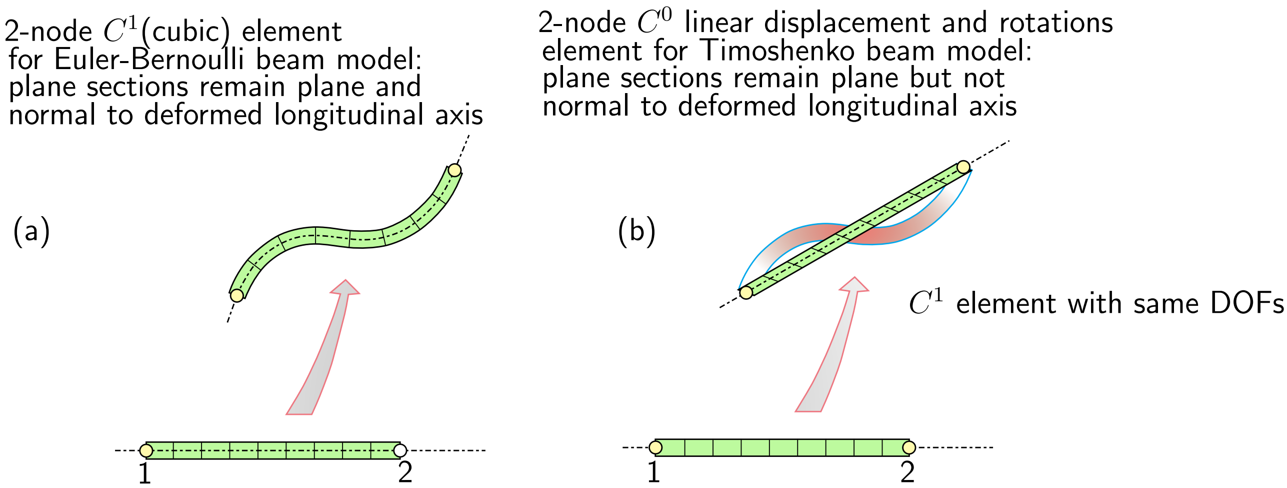


*Figure 1.6: Contrasting kinematics of 2-node beam FEM models based on (a) Euler-Bernoulli beam theory, and (b) Timoshenko beam theory. These are called $C^1$ and $C^0$ beam elements, respectively, in the FEM literature.*

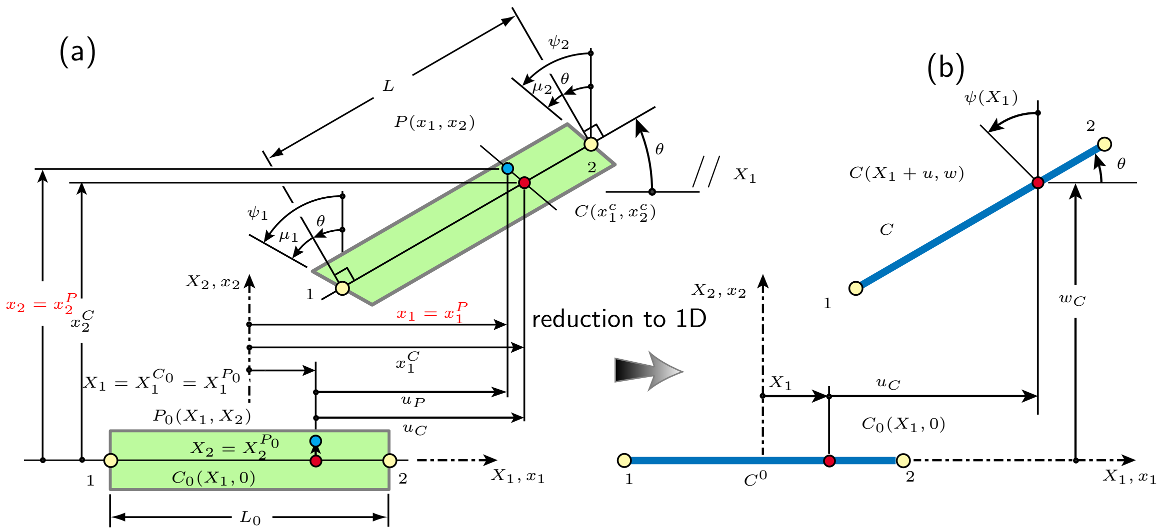


*Figure 1.7: Lagrangian kinematics of $C^0$ beam element with $X_1$-aligned reference configuration: (a) plane beam moving as a 2D body; (b) reduction of motion description to 1D as measured by coordinate $X_1$.*

by the area integrals

$$A_0 = \int_{A_0} dA, \qquad \int_{A_0} X_2 dA = 0, \qquad I_0 = \int_{A_0} (X_2)^2 dA \tag{1.1}$$

In the current configuration those quantities become $A$, $I$ and $L$, respectively, but only the current length $L$ is frequently used in the Total Langrange formulation. The material remains linearly elastic, with Young's modulus $E$ and shear modulus $G$.

The element has the six degrees of freedom depicted in Figure 1.4. These degrees of freedom are collected in the node displacement

$$\boldsymbol{u_1} = \begin{bmatrix} u_1 \\ w_1 \\ \psi_1 \end{bmatrix}, \qquad \boldsymbol{u_2} = \begin{bmatrix} u_2 \\ w_2 \\ \psi_2 \end{bmatrix} \tag{1.2}$$

### 1.2.2 Motion

In this section, the kinematic of the Timoshenko model element have been clarified and the kinematic of the Bernoulli model element will be discussed in Chapter 4. Basically Timoshenko model element state that cross sections remain plane upon deformation, but not necessarily normal to the deformed longitudinal axis. In addition, changes in cross section geometry are neglected. It means, cross sectional area $A$ and shear area $\hat{A}$ remain constant.
To work out the Lagrangian kinematics of the element shown in Figure 1.7(a), we study the motion of a generic particle located at $P0(X_1, X_2)$ in the reference configuration, which moves to $P(x_1, x_2)$ in the current configuration. The projections of $P_0$ and $P$ on the neutral axis, along the cross sections at $C^0$ and $C$ are called $C^1(X_1, 0)$ and $C(x_1^c, x_2^c)$, respectively. The exact kinematics is

$$\begin{bmatrix} x_1 \\ x_2 \end{bmatrix} = \begin{bmatrix} x_1^c - X_2(\sin\theta + \sin\mu\cos\theta) \\ x_2^c + X_2(\cos\theta - \sin\mu\sin\theta) \end{bmatrix} = \begin{bmatrix} x_1^c - X_2[\sin\psi + (1-\cos\mu)\sin\theta] \\ x_2^c + X_2[\cos\psi + (1-\cos\mu)\cos\theta] \end{bmatrix} \tag{1.3}$$

in which $\theta + \mu$ has been replaced by $\psi$. But $x_1^C = X_1 + u_C$ and $x_2^C = w_C$. From now we denote $u_C$ and $w_C$ simply as $u$ and $w$, respectively. Assume for simplicity that $\mu$ is constant over the element. Expand (1.3) in Taylor series in $\mu$ up to $O(\mu^4)$:

$$\begin{bmatrix} x_1 \\ x_2 \end{bmatrix} = \begin{bmatrix} u + X_1 + \frac{1}{2}X_2\mu^3\cos\psi - X_2(1 + \frac{1}{2}\mu^2 + \frac{7}{24}\mu^4)\sin\psi \\ w + X_2(1 + \frac{1}{2}\mu^2 - \frac{7}{24}\mu^4)\cos\psi + \frac{1}{2}X_2\mu^3\sin\psi \end{bmatrix} \tag{1.4}$$

If we assume the shear distortion is very small, setting $\mu \to 0$ in (1.4) gives the simplified Lagrangian description of the motion

$$\begin{bmatrix} x_1 \\ x_2 \end{bmatrix} = \begin{bmatrix} u + X_1 - X_2\sin\psi \\ w + X_2\cos\psi \end{bmatrix} \tag{1.5}$$

in which $u$, $w$ and $\psi$ are functions of $X_1$ only.

### 1.2.3 Strain-Displacement Relations

The deformation gradient matrix of the motion (1.5) is

$$\boldsymbol{F} = \begin{bmatrix} \frac{\partial x_1}{\partial X_1} & \frac{\partial x_1}{\partial X_2} \\ \frac{\partial x_2}{\partial X_1} & \frac{\partial x_2}{\partial X_2} \end{bmatrix} = \begin{bmatrix} 1 + u' - X_2\kappa\cos\psi & -\sin\psi \\ w' - X_2\kappa\sin\psi & \cos\psi \end{bmatrix} \tag{1.6}$$

in which primes denote derivatives with respect to $X_1$, and $\kappa = \psi'$ is the curvature. The displacement gradient matrix is

$$\boldsymbol{G} = \boldsymbol{F} - \boldsymbol{I} = \begin{bmatrix} u' - X_2\kappa\cos\psi & -\sin\psi \\ w' - X_2\kappa\sin\psi & \cos\psi - 1 \end{bmatrix} \tag{1.7}$$

the plane portion of the Green-Lagrange (GL) strain tensor follows as

$$\boldsymbol{E} = \begin{bmatrix} E_{11} & E_{12} \\ E_{21} & E_{22} \end{bmatrix} = \frac{1}{2}(\boldsymbol{F}^T\boldsymbol{F} - \boldsymbol{I}) = \frac{1}{2}(\boldsymbol{G} + \boldsymbol{G}^T) + \frac{1}{2}\boldsymbol{G}^T\boldsymbol{G} \tag{1.8}$$

This expands to the component form

$$\boldsymbol{E} = \frac{1}{2}\begin{bmatrix} 2(u' - X_2\kappa\cos\psi) + (u' - X_2\kappa\cos\psi)^2 + (w' - X_2\kappa\sin\psi)^2 & -(1+u')\sin\psi + w'\cos\psi \\ -(1+u')\sin\psi + w'\cos\psi & 0 \end{bmatrix} \tag{1.9}$$

It is seen that the only nonzero strains are the axial strain $E_{11}$ and the shear strain $E_{12}+E_{21} = 2E_{12}$, whereas $E_{22}$ vanishes. Through the consistent-linearization described in next section, it can be shown that under the small-strain assumptions made precise therein, the axial strain $E_{11}$ can be replaced by the simpler form

$$E_{11} = (1+u')\cos\psi + w'\sin\psi - X_2\kappa - 1 \tag{1.10}$$

in which all quantities appear linearly except $\psi$. The nonzero axial and shear strains will be arranged in the strain vector

$$\boldsymbol{E} = \begin{bmatrix} E_1 \\ E_2 \end{bmatrix} = \begin{bmatrix} E_{11} \\ 2E_{12} \end{bmatrix} = \begin{bmatrix} (1+u')\cos\psi + w'\sin\psi - X_2\kappa - 1 \\ -(1+u')\sin\psi + w'\cos\psi \end{bmatrix} = \begin{bmatrix} \epsilon - X_2\kappa \\ \gamma \end{bmatrix} \tag{1.11}$$

The three strain quantities introduced in (1.11)

$$\boxed{\begin{aligned} &\epsilon = (1+u').\cos\psi + w'.\sin\psi - 1, \\ &\gamma = w'.\cos\psi - (1+u').\sin\psi, \\ &\kappa = \psi' \end{aligned}} \tag{1.12}$$

### 1.2.4 Consistent Linearization

Based on the polar decomposition analysis of the deformation gradient, the consistent linearization (1.10) can be derived.Fist introduce an orthogonal matrix

$$\boldsymbol{\Omega}(\alpha) = \begin{bmatrix} \cos\alpha & -\sin\alpha \\ \sin\alpha & \cos\alpha \end{bmatrix} \tag{1.13}$$

which represents a two-dimensional rotation (about $X_3$) through an angle $\alpha$. Since $\boldsymbol{\Omega}$ is an orthogonal matrix, $\boldsymbol{\Omega}^T = \boldsymbol{\Omega}^{-1}$. Then matrix $\boldsymbol{R}$ can be introduced

$$\boldsymbol{\Omega}(-\psi) = \boldsymbol{R} = \begin{bmatrix} \cos\psi & \sin\psi \\ -\sin\psi & \cos\psi \end{bmatrix} \tag{1.14}$$

Premultiplying (1.6) by $R$ gives the modified deformation gradient

$$\bar{\boldsymbol{F}} = \boldsymbol{R}\boldsymbol{F} = \begin{bmatrix} (1+u')\cos\psi + w'\sin\psi - X_2\kappa & 0 \\ -(1+u')\sin\psi + w'\cos\psi & 1 \end{bmatrix} \tag{1.15}$$

for linearization purpose matrix $L$ will be defined

$$\boldsymbol{L} = \bar{\boldsymbol{F}} - \boldsymbol{I} = \begin{bmatrix} (1+u')\cos\psi + w'\sin\psi - X_2\kappa - 1 & 0 \\ -(1+u')\sin\psi + w'\cos\psi & 0 \end{bmatrix} \tag{1.16}$$

Also it can be written that $\boldsymbol{F} = \boldsymbol{R}^{-1}\bar{\boldsymbol{F}} = \boldsymbol{R}^T\bar{\boldsymbol{F}}$, then Green Lagrange tensor in Equation (1.8) can be rewritten as

$$\begin{aligned} \boldsymbol{E} &= \frac{1}{2}(\boldsymbol{F}^T\boldsymbol{F} - \boldsymbol{I}) = \frac{1}{2}[(\boldsymbol{R}^T\bar{\boldsymbol{F}})^T(\boldsymbol{R}^T\bar{\boldsymbol{F}}) - \boldsymbol{I}] \\ &= \frac{1}{2}[\bar{\boldsymbol{F}}^T\boldsymbol{R}\boldsymbol{R}^T\bar{\boldsymbol{F}} - \boldsymbol{I}] \\ &= \frac{1}{2}[\bar{\boldsymbol{F}}^T\boldsymbol{R}\boldsymbol{R}^{-1}\bar{\boldsymbol{F}} - \boldsymbol{I}] \\ &= \frac{1}{2}[\bar{\boldsymbol{F}}^T\bar{\boldsymbol{F}} - \boldsymbol{I}] \end{aligned} \tag{1.17}$$

By inserting $\bar{\boldsymbol{F}} = \boldsymbol{L} + \boldsymbol{I}$ and $\bar{\boldsymbol{F}}^T = \boldsymbol{L}^T + \boldsymbol{I}$ in Equation (1.17) we obtain

$$\begin{aligned} \boldsymbol{E} &= \frac{1}{2}(\boldsymbol{L}^T + \boldsymbol{I})(\boldsymbol{L} + \boldsymbol{I}) - \boldsymbol{I} \\ &= \frac{1}{2}(\boldsymbol{L}^T\boldsymbol{L} + \boldsymbol{L}^T + \boldsymbol{L} + \boldsymbol{I} - \boldsymbol{I}) \\ &= \frac{1}{2}(\boldsymbol{L}^T + \boldsymbol{L} + \boldsymbol{L}^T\boldsymbol{L}) \end{aligned} \tag{1.18}$$

The higher order term $\boldsymbol{L}^T\boldsymbol{L}$ can be neglected because it is assumed that strains remain small therefore $\frac{L}{L_0} - 1$, $X_2\kappa$ and $\bar{\mu} = -\mu = \theta - \psi$ are small quantities. It follows that

$$\boldsymbol{E} = \frac{1}{2}(\boldsymbol{L}^T + \boldsymbol{L}) = \begin{bmatrix} (1+u')\cos\psi + w'\sin\psi - X_2\kappa - 1 & -(1+u')\sin\psi + w'\cos\psi \\ -(1+u')\sin\psi + w'\cos\psi & 0 \end{bmatrix} \tag{1.19}$$

Carrying out this linearization one finds that $E_{12}$ and $E_{22}$ do not change from Equation (1.9), but that $E_{11}$ simplifies to (1.10).

# Chapter 2

# Geometically Exact Beam Theory

## 2.1 Kinematics

The associated Strain–Displacement relations were derived in previous chapter. This leads to strain measures for the axial strain $\epsilon$, the shear strain $\gamma$ and the curvature $\kappa$:

$$\begin{aligned}
&\epsilon(X_1) = (1 + u'(X_1)).\cos\psi(X_1) + w'(X_1).\sin\psi(X_1) - 1,\\
&\gamma(X_1) = w'(X_1).\cos\psi(X_1) - (1 + u'(X_1)).\sin\psi(X_1),\\
&\kappa(X_1) = \psi'(X_1)
\end{aligned} \tag{2.1}$$

with
$u$: axial displacement
$w$: transverse displacement
$\psi$: rotation

$\epsilon$: axial strain
$\gamma$: shear strain
$\kappa$: curvature

$u'$: derivative of axial displacement with respect to $X_1$ coordinate
$w'$: derivative of transverse displacement with respect to $X_1$ coordinate
$\psi'$: derivative of rotation with respect to $X_1$ coordinate

Note that the strain (2.1) for the curvature is linear in $\psi$. The strain measures can also be formulated in matrix notation:

$$\boldsymbol{\epsilon}(X_1) = \boldsymbol{T}(\psi).\boldsymbol{u}'(X_1) - \boldsymbol{\Psi}$$

$$\boldsymbol{\epsilon} = \begin{bmatrix} \epsilon \\ \gamma \\ \kappa \end{bmatrix}, \boldsymbol{T}(\psi) = \begin{bmatrix} \cos\psi & \sin\psi & 0 \\ -\sin\psi & \cos\psi & 0 \\ 0 & 0 & 1 \end{bmatrix}, \boldsymbol{u}' = \begin{bmatrix} u' \\ w' \\ \psi' \end{bmatrix}, \boldsymbol{\Psi} = \begin{bmatrix} 1-\cos\psi \\ \sin\psi \\ 0 \end{bmatrix} \tag{2.2}$$

Relation (2.2) shows the simple structure of non-linear strain measures. The nonlinearity is only associated with the $\sin$ and $\cos$ functions in which the rotation angle $\psi$ occurs. These act on $u$ and $w$ by the rotation matrix $\boldsymbol{T}$.

## 2.2 Weak Form of Equilibrium

The weak form of equilibrium, which is equivalent to the principle of virtual work, can be stated for shear elastic beams as

$$G(u,\eta) = \int_0^l \delta\boldsymbol{\epsilon}^T(X_1).\boldsymbol{S}dx - \int_0^l \boldsymbol{\eta}^T(X_1).\boldsymbol{q}dx = 0 \tag{2.3}$$

After extracting the above equation, we obtain

$$\begin{gathered} G(u,\eta) = \int_0^l (N.\delta\epsilon + Q.\delta\gamma + M.\delta\kappa)dx - \int_0^l (n.\delta u + q.\delta w)dx = 0 \\ \text{with } \boldsymbol{S} = \begin{bmatrix} N \\ Q \\ M \end{bmatrix}, \delta\boldsymbol{\epsilon} = \begin{bmatrix} \delta\epsilon \\ \delta\gamma \\ \delta\kappa \end{bmatrix}, \boldsymbol{\eta} = \begin{bmatrix} \delta u \\ \delta w \\ \delta\psi \end{bmatrix}, \boldsymbol{q} = \begin{bmatrix} n \\ q \\ 0 \end{bmatrix} \end{gathered} \tag{2.4}$$

It is clear that $N$ ,$Q$ ,$M$ are the stress resultants, and $n$ and $q$, respectively, are the loading in axial and perpendicular direction related to the beam axis. The strains vector $\boldsymbol{\epsilon}$ comes from the definition given in (2.1). For the geometrically exact model, the virtual strains from (2.1) yields

$$\begin{aligned} &\delta\epsilon = \delta u'.\cos\psi - (1+u').\delta\psi.\sin\psi + \delta w'.\sin\psi + w'.\delta\psi.\cos\psi \\ &\delta\gamma = \delta w'.\cos\psi - w'.\delta\psi.\sin\psi - \delta u'.\sin\psi - (1+u').\delta\psi.\cos\psi \\ &\delta\kappa = \delta\psi' \end{aligned} \tag{2.5}$$

and in Matrix form it can be written

$$\begin{gathered} \delta\boldsymbol{\epsilon}(X_1) = \boldsymbol{T}(\psi).\boldsymbol{\eta}'(X_1) + \frac{\partial\boldsymbol{T}(\psi)}{\partial\psi}.\boldsymbol{u}'(X_1).\delta\psi - \frac{\partial\boldsymbol{\Psi}(\psi)}{\partial\psi}.\delta\psi \\ \boldsymbol{\eta}' = \begin{bmatrix} \delta u' \\ \delta w' \\ \delta\psi' \end{bmatrix}, \frac{\partial\boldsymbol{T}(\psi)}{\partial\psi} = \begin{bmatrix} -\sin\psi & \cos\psi & 0 \\ -\cos\psi & -\cos\psi & 0 \\ 0 & 0 & 0 \end{bmatrix}, \frac{\partial\boldsymbol{\Psi}(\psi)}{\partial\psi} = \begin{bmatrix} \sin\psi \\ \cos\psi \\ 0 \end{bmatrix} \end{gathered} \tag{2.6}$$

By inserting this relation in the weak form (2.4), the first term can be specified as

$$\int_0^l \delta\boldsymbol{\epsilon}^T(X_1).\boldsymbol{S}dx = \int_0^l \Big[\boldsymbol{\eta}'^T(X_1).\boldsymbol{T}^T(\psi) + \delta\psi.\boldsymbol{u}'^T(X_1).(\frac{\partial\boldsymbol{T}(\psi)}{\partial\psi})^T - \delta\psi.(\frac{\partial\boldsymbol{\Psi}(\psi)}{\partial\psi})^T\Big].\boldsymbol{S}dx \tag{2.7}$$

This is the stress divergence term of the geometrically exact beam model. This weak form represents a non-linear functional with respect to the displacements and rotations. Since analytic solutions are only available for special cases, the finite element method will be applied to solve.

## 2.3 Constitutive Equations

Within the simulation of beam structures, it can be assumed for most applications that the strain are small (See section 1.2.4), even for large deflections and rotations. Hence it is possible to describe elastic material behavior by the classical Hooke law of the linear theory. Therefore the stress resultants leading to the compact form

$$\boldsymbol{S} = \boldsymbol{D}.\boldsymbol{\epsilon}$$

$$\boldsymbol{S} = \begin{bmatrix} EA & 0 & 0 \\ 0 & G\hat{A} & 0 \\ 0 & 0 & EI \end{bmatrix} \cdot \begin{bmatrix} \epsilon \\ \gamma \\ \kappa \end{bmatrix} \tag{2.8}$$

with Young modulus $E$, the shear modulus $G$, the cross sectional area $A$ and the moment of inertia $I$. The introduction of the shear area $\hat{A}$ is related to a shear correction term which is needed within to correct the violation of the boundary condition for the shear stresses at $X_2 = \pm h/2$ ($h$ is thickness) due to the beam model assumption of plane sections remain plane.

## 2.4 Finite Element Formulation

For the finite element discretization of the shear elastic geometrically exact beam model linear shape functions can be selected since the weak form needs only shape functions which are $C^0$-continuous. Hence polynomials (2.9) or (2.10) can be applied as finite element interpolations for the axial displacements $u$, the deflection $w$ and the rotation $\psi$.

▷ Linear shape functions and corresponded derivation:

$$\begin{aligned} N_1(\xi_1) &= \frac{1}{2}(1-\xi_1) & \qquad N_1'(\xi_1) &= -\frac{1}{2} \\ N_2(\xi_1) &= \frac{1}{2}(1+\xi_1) & \qquad N_2'(\xi_1) &= \frac{1}{2} \end{aligned} \tag{2.9}$$

▷ Quadratic shape functions and corresponded derivation:

$$\begin{aligned} N_1(\xi_1) &= \frac{1}{2}\xi_1(\xi_1-1) & \qquad N_1'(\xi_1) &= \xi_1 - \frac{1}{2} \\ N_2(\xi_1) &= (1-\xi_1^2) & \qquad N_2'(\xi_1) &= -2\xi_1 \\ N_3(\xi_1) &= \frac{1}{2}\xi_1(\xi_1+1) & \qquad N_3'(\xi_1) &= \xi_1 + \frac{1}{2} \end{aligned} \tag{2.10}$$

Computations show that elements with quadratic shape functions yield better approximations of the solutions than linear ones. Mathematically this leads to a higher convergence order. This is supported by convergence analysis of the linear case. Quadratic interpolations are based on elements with three nodes. The nodal value vector can be defined (See section 1.2.1)

$$\boldsymbol{u}_I = \begin{bmatrix} u_I & w_I & \psi_I \end{bmatrix}^T, \boldsymbol{u}_I' = 0 \tag{2.11}$$

For deriving the finite element formulation of weak form there will be needed vector variables like $\boldsymbol{u}_e$, $\boldsymbol{u}'_e$, $\boldsymbol{\epsilon}_e$, $\delta\boldsymbol{u}_e$, $\delta\boldsymbol{u}'_e$ and $\delta\boldsymbol{\epsilon}_e$ which have to be interpolated and expressed based on desired shape functions. In these expressions all the shape functions are in $X_1$ coordination and subscript $e$ refers to one element.

### 2.4.1 Displacement $\boldsymbol{u}_e$

The displacement vector of an element $\boldsymbol{u}_e$ with shape function can be interpolated

$$
\begin{aligned}
u_e &= \sum_{I=1}^{n=3} N_I(X_1).u_I = N_1(X_1).u_1 + N_2(X_1).u_2 + N_3(X_1).u_3 \\
w_e &= \sum_{I=1}^{n=3} N_I(X_1).w_I = N_1(X_1).w_1 + N_2(X_1).w_2 + N_3(X_1).w_3 \\
\psi_e &= \sum_{I=1}^{n=3} N_I(X_1).\psi_I = N_1(X_1).\psi_1 + N_2(X_1).\psi_2 + N_3(X_1).\psi_3
\end{aligned}
\tag{2.12}
$$

and the Matrix form

$$
\boxed{
\begin{aligned}
&\boldsymbol{u}_e = \sum_{I=1}^{n=3} [\boldsymbol{N}_I.\boldsymbol{u}_I] \\
&\begin{bmatrix} u_e \\ w_e \\ \psi_e \end{bmatrix} = \sum_{I=1}^{n=3} \begin{bmatrix} N_I(X_1) & 0 & 0 \\ 0 & N_I(X_1) & 0 \\ 0 & 0 & N_I(X_1) \end{bmatrix} \cdot \begin{bmatrix} u_I \\ w_I \\ \psi_I \end{bmatrix}
\end{aligned}
}
\tag{2.13}
$$

### 2.4.2 Derivation of Displacement $\boldsymbol{u}'_e$

The derivation of displacement vector of an element $\boldsymbol{u}'_e$ with shape function can be interpolated

$$
\begin{aligned}
u'_e &= \sum_{I=1}^{n=3} N'_I(X_1).u_I = N'_1(X_1).u_1 + N'_2(X_1).u_2 + N'_3(X_1).u_3 \\
w'_e &= \sum_{I=1}^{n=3} N'_I(X_1).w_I = N'_1(X_1).w_1 + N'_2(X_1).w_2 + N'_3(X_1).w_3 \\
\psi'_e &= \sum_{I=1}^{n=3} N'_I(X_1).\psi_I = N'_1(X_1).\psi_1 + N'_2(X_1).\psi_2 + N'_3(X_1).\psi_3
\end{aligned}
\tag{2.14}
$$

and the Matrix form

$$\boxed{\begin{aligned}\boldsymbol{u}'_e &= \sum_{I=1}^{n=3} [\boldsymbol{N}'_I.\boldsymbol{u}_I] \\ \begin{bmatrix} u'_e \\ w'_e \\ \psi'_e \end{bmatrix} &= \sum_{I=1}^{n=3} \begin{bmatrix} N'_I(X_1) & 0 & 0 \\ 0 & N'_I(X_1) & 0 \\ 0 & 0 & N'_I(X_1) \end{bmatrix} \cdot \begin{bmatrix} u_I \\ w_I \\ \psi_I \end{bmatrix}\end{aligned}} \tag{2.15}$$

## 2.4.3 Strain $\boldsymbol{\epsilon}_e$

The strain vector of an element $\boldsymbol{\epsilon}_e$ with shape function can be interpolated by inserting equation (2.15) in (2.1). Thus

$$\begin{aligned}
\epsilon_e &= (1 + \sum_{I=1}^{n=3} N'_I(X_1).u_I).\cos\psi_e + (\sum_{I=1}^{n=3} N'_I(X_1).w_I).\sin\psi_e - 1, \\
\gamma_e &= (\sum_{I=1}^{n=3} N'_I(X_1).w_I).\cos\psi_e - (1 + \sum_{I=1}^{n=3} N'_I(X_1).u_I).\sin\psi_e, \\
\kappa_e &= \sum_{I=1}^{n=3} N'_I(X_1).\psi_I
\end{aligned} \tag{2.16}$$

and the matrix form can be derived

$$\begin{bmatrix} \epsilon_e \\ \gamma_e \\ \kappa_e \end{bmatrix} = \begin{bmatrix} \cos\psi_e & \sin\psi_e & 0 \\ -\sin\psi_e & \cos\psi_e & 0 \\ 0 & 0 & 1 \end{bmatrix} \cdot \begin{bmatrix} \sum_{I=1}^{n=3} N'_I(X_1).u_I \\ \sum_{I=1}^{n=3} N'_I(X_1).w_I \\ \sum_{I=1}^{n=3} N'_I(X_1).\psi_I \end{bmatrix} - \begin{bmatrix} 1-\cos\psi \\ \sin\psi \\ 0 \end{bmatrix} \tag{2.17}$$

and drawing out the summation symbol and arrange it we obtain

$$\begin{bmatrix} \epsilon_e \\ \gamma_e \\ \kappa_e \end{bmatrix} = \begin{bmatrix} \cos\psi_e & \sin\psi_e & 0 \\ -\sin\psi_e & \cos\psi_e & 0 \\ 0 & 0 & 1 \end{bmatrix} \cdot \sum_{I=1}^{n=3} \left[ \begin{bmatrix} N'_I(X_1) & 0 & 0 \\ 0 & N'_I(X_1) & 0 \\ 0 & 0 & N'_I(X_1) \end{bmatrix} \cdot \begin{bmatrix} u_I \\ w_I \\ \psi_I \end{bmatrix} \right] - \begin{bmatrix} 1-\cos\psi \\ \sin\psi \\ 0 \end{bmatrix} \tag{2.18}$$

which shortly we can express it like below.

$$\boxed{\begin{aligned} \boldsymbol{\epsilon}_e &= \boldsymbol{T}(\psi_e).\sum_{I=1}^{n=3}[\boldsymbol{N'}_I.\boldsymbol{u}_I] - \boldsymbol{\Psi} \\ \boldsymbol{N'}_I(X_1) &= \begin{bmatrix} N'_I(X_1) & 0 & 0 \\ 0 & N'_I(X_1) & 0 \\ 0 & 0 & N'_I(X_1) \end{bmatrix} \end{aligned}} \tag{2.19}$$

## 2.4.4 Virtual Displacement $\delta\boldsymbol{u}_e$

The virtual displacement vector of an element $\delta\boldsymbol{u}_e$ with shape function can be interpolated

$$\begin{aligned} \delta u_e &= \sum_{I=1}^{n=3} N_I(X_1).\delta u_I = N_1(X_1).\delta u_1 + N_2(X_1).\delta u_2 + N_3(X_1).\delta u_3 \\ \delta w_e &= \sum_{I=1}^{n=3} N_I(X_1).\delta w_I = N_1(X_1).\delta w_1 + N_2(X_1).\delta w_2 + N_3(X_1).\delta w_3 \\ \delta \psi_e &= \sum_{I=1}^{n=3} N_I(X_1).\delta \psi_I = N_1(X_1).\delta \psi_1 + N_2(X_1).\delta \psi_2 + N_3(X_1).\delta \psi_3 \end{aligned} \tag{2.20}$$

and the matrix form is

$$\boxed{\begin{aligned} &\delta\boldsymbol{u}_e = \sum_{I=1}^{n=3}[\boldsymbol{N}_I.\boldsymbol{\eta}_I] \\ &\begin{bmatrix} \delta u_e \\ \delta w_e \\ \delta \psi_e \end{bmatrix} = \sum_{I=1}^{n=3} \begin{bmatrix} N_I(X_1) & 0 & 0 \\ 0 & N_I(X_1) & 0 \\ 0 & 0 & N_I(X_1) \end{bmatrix} \cdot \begin{bmatrix} \delta u_I \\ \delta w_I \\ \delta \psi_I \end{bmatrix} \end{aligned}} \tag{2.21}$$

## 2.4.5 Derivation of Virtual Displacement $\delta\boldsymbol{u}'_e$

The derivation of virtual displacement vector of an element $\delta\boldsymbol{u}'_e$ with shape function can be interpolated

$$\begin{aligned} \delta u'_e &= \sum_{I=1}^{n=3} N'_I(X_1).\delta u_I = N'_1(X_1).\delta u_1 + N'_2(X_1).\delta u_2 + N'_3(X_1).\delta u_3 \\ \delta w'_e &= \sum_{I=1}^{n=3} N'_I(X_1).\delta w_I = N'_1(X_1).\delta w_1 + N'_2(X_1).\delta w_2 + N'_3(X_1).\delta w_3 \\ \delta \psi'_e &= \sum_{I=1}^{n=3} N'_I(X_1).\delta \psi_I = N'_1(X_1).\delta \psi_1 + N'_2(X_1).\delta \psi_2 + N'_3(X_1).\delta \psi_3 \end{aligned} \tag{2.22}$$

and the matrix form is

$$\boxed{\begin{aligned} &\delta \boldsymbol{u}'_e = \sum_{I=1}^{n=3} [\boldsymbol{N}'_I . \boldsymbol{\eta}_I] \\ &\begin{bmatrix} \delta u'_e \\ \delta w'_e \\ \delta \psi'_e \end{bmatrix} = \sum_{I=1}^{n=3} \begin{bmatrix} N'_I(X_1) & 0 & 0 \\ 0 & N'_I(X_1) & 0 \\ 0 & 0 & N'_I(X_1) \end{bmatrix} \cdot \begin{bmatrix} \delta u_I \\ \delta w_I \\ \delta \psi_I \end{bmatrix} \end{aligned}} \tag{2.23}$$

### 2.4.6 Virtual Strain $\delta \boldsymbol{\epsilon}_e$

The virtual strain vector of an element $\delta \boldsymbol{\epsilon}_e$ with shape function can be interpolated

$$\begin{aligned} \delta \epsilon_e &= \delta u'_e . \cos \psi_e - (1 + u'_e) . \delta \psi_e . \sin \psi_e + \delta w'_e . \sin \psi_e + w'_e . \delta \psi_e . \cos \psi_e \\ \rightarrow \delta \epsilon_e &= (\sum_{I=1}^{n=3} N'_I(X_1) . \delta u_I) . \cos \psi_e + (\sum_{I=1}^{n=3} N'_I(X_1) . \delta w_I) . \sin \psi_e + \\ &\quad (\sum_{I=1}^{n=3} N_I(X_1) . \delta \psi_I) . \underbrace{(-(1 + u'_e) . \sin \psi_e + w'_e . \cos \psi_e)}_{\alpha_e} \end{aligned} \tag{2.24}$$

$$\begin{aligned} \delta \gamma_e &= \delta w'_e . \cos \psi_e - w'_e . \delta \psi_e . \sin \psi_e - \delta u'_e . \sin \psi_e - (1 + u'_e) . \delta \psi_e . \cos \psi_e \\ \rightarrow \delta \gamma_e &= -(\sum_{I=1}^{n=3} N'_I(X_1) . \delta u_I) . \sin \psi_e + (\sum_{I=1}^{n=3} N'_I(X_1) . \delta w_I) . \cos \psi_e + \\ &\quad (\sum_{I=1}^{n=3} N_I(X_1) . \delta \psi_I) . \underbrace{(-(1 + u'_e) . \cos \psi_e - w'_e . \sin \psi_e)}_{\beta_e} \end{aligned} \tag{2.25}$$

$$\delta \kappa_e = \delta \psi'_e = \sum_{I=1}^{n=3} N'_I(X_1) . \delta \psi_I \tag{2.26}$$

and the matrix form is

$$\begin{bmatrix} \delta \epsilon_e \\ \delta \gamma_e \\ \delta \kappa_e \end{bmatrix} = \sum_{I=1}^{n=3} \begin{bmatrix} N'_I(X_1) . \cos \psi_e & N'_I(X_1) . \sin \psi_e & N_I(X_1) . \alpha_e \\ -N'_I(X_1) . \sin \psi_e & N'_I(X_1) . \cos \psi_e & N_I(X_1) . \beta_e \\ 0 & 0 & N'_I(X_1) \end{bmatrix} \cdot \begin{bmatrix} \delta u_I \\ \delta w_I \\ \delta \psi_I \end{bmatrix} \tag{2.27}$$

and shortly we can write

$$\boxed{\begin{aligned} \delta\boldsymbol{\epsilon}_e &= \sum_{I=1}^{n=3}[\boldsymbol{B}_I.\boldsymbol{\eta}_I] \\ \boldsymbol{B}_I(X_1) &= \begin{bmatrix} N_I'(X_1).\cos\psi_e & N_I'(X_1).\sin\psi_e & N_I(X_1).\alpha_e \\ -N_I'(X_1).\sin\psi_e & N_I'(X_1).\cos\psi_e & N_I(X_1).\beta_e \\ 0 & 0 & N_I'(X_1) \end{bmatrix} \end{aligned}} \tag{2.28}$$

## 2.5 Weak Form in terms of Nodal Quantities $\boldsymbol{u}_I$

By inserting the equation (2.28) in the stress divergence term, the weak form (2.7) can be completely expressed by the displacements and rotations after inserting the constitutive equation (2.8).
This completes the formulation of the different finite element models for non-linear beams since the stress resultants in (2.4) can be obtained via the material equation (2.18) in terms of the nodal quantities $\boldsymbol{u}_I$. Generally, this leads to the non-linear equation system. Equation (2.3) can be expressed discretely

$$G(u,\eta) = \bigcup_{j=1}^{n_e}\Big[\int_0^{L_e}(N_e.\delta\epsilon_e + Q_e.\delta\gamma_e + M_e.\delta\kappa_e)dx - \int_0^{L_e}(n_e.\delta u_e + q_e.\delta w_e)dx\Big] = 0 \tag{2.29}$$

By inserting (2.24)[2] in $\delta\epsilon_e$, (2.25)[2] in $\delta\gamma_e$, (2.26) in $\delta\kappa_e$, (2.20)[1] in $\delta u_e$ and (2.20)[2] in $\delta w_e$ we obtain

$$\begin{aligned} G(u,\eta) = &\bigcup_{j=1}^{n_e}\Big[\int_0^{L_e}\Big[N_e.((\sum_{I=1}^{n=3}N_I'(X_1).\delta u_I).\cos\psi_e + (\sum_{I=1}^{n=3}N_I'(X_1).\delta w_I).\sin\psi_e + \\ &(\sum_{I=1}^{n=3}N_I(X_1).\delta\psi_e).\alpha_e) + Q_e.((\sum_{I=1}^{n=3}N_I'(X_1).\delta w_I).\cos\psi_e - (\sum_{I=1}^{n=3}N_I'(X_1).\delta u_I).\sin\psi_e + \\ &(\sum_{I=1}^{n=3}N_I(X_1).\delta\psi_e).\beta_e) + M_e.(\sum_{I=1}^{n=3}N_I'(X_1).\delta\psi_e)\Big]dX_1 - \int_0^{L_e}\Big[n_e.(\sum_{I=1}^{n=3}N_I(X_1).\delta u_I) + \\ &q_e.(\sum_{I=1}^{n=3}N_I(X_1).\delta w_I)\Big]dX_1\Big] = 0 \end{aligned} \tag{2.30}$$

The summation symbol is drown out

$$
\begin{aligned}
G(u,\eta) =& \bigcup_{j=1}^{n_e}\Big[\Big[N_e.(\sum_{I=1}^{n=3}\delta u_I.\int_0^{L_e}(N_I'(X_1).\cos\psi_e)dX_1+\sum_{I=1}^{n=3}\delta w_I.\int_0^{L_e}(N_I'(X_1).\sin\psi_e)dX_1+\\
&\sum_{I=1}^{n=3}\delta\psi_I.\int_0^{L_e}(N_I(X_1).\alpha_e)dX_1)+Q_e.(\sum_{I=1}^{n=3}\delta w_I.\int_0^{L_e}(N_I'(X_1).\cos\psi_e)dX_1-\\
&\sum_{I=1}^{n=3}\delta u_I.\int_0^{L_e}(N_I'(X_1).\sin\psi_e)dX_1+\sum_{I=1}^{n=3}\delta\psi_I.\int_0^{L_e}(N_I(X_1).\beta_e)dX_1)+\\
&M_e.(\sum_{I=1}^{n=3}\delta\psi_I.\int_0^{L_e}N_I'(X_1)dX_1)\Big]-\Big[n_e.(\sum_{I=1}^{n=3}\delta u_I.\int_0^{L_e}N_I(X_1)dX_1)+\\
&q_e.(\sum_{I=1}^{n=3}\delta w_I.\int_0^{L_e}N_I(X_1)dX_1)+\underbrace{m_e}_{=0}.(\sum_{I=1}^{n=3}\delta\psi_I.\int_0^{L_e}N_I(X_1)dX_1)\Big]\Big]=0.
\end{aligned}
\tag{2.31}
$$

Then we transform it from physical coordination to natural coordination

$$
\begin{aligned}
G(u,\eta) =& \bigcup_{j=1}^{n_e}\Big[\Big[N_e.(\sum_{I=1}^{n=3}\delta u_I.\int_{-1}^{+1}(N_I'(\xi).\cos\psi_e.\frac{L_e}{2})d\xi+\sum_{I=1}^{n=3}\delta w_I.\int_{-1}^{+1}(N_I'(\xi).\sin\psi_e.\frac{L_e}{2})d\xi+\\
&\sum_{I=1}^{n=3}\delta\psi_I.\int_{-1}^{+1}(N_I(\xi).\alpha_e.\frac{L_e}{2})d\xi)+Q_e.(\sum_{I=1}^{n=3}\delta w_I.\int_{-1}^{+1}(N_I'(\xi).\cos\psi_e.\frac{L_e}{2})d\xi-\\
&\sum_{I=1}^{n=3}\delta u_I.\int_{-1}^{+1}(N_I'(\xi).\sin\psi_e.\frac{L_e}{2})d\xi+\sum_{I=1}^{n=3}\delta\psi_I.\int_{-1}^{+1}(N_I(\xi).\beta_e.\frac{L_e}{2})d\xi)+\\
&M_e.(\sum_{I=1}^{n=3}\delta\psi_I.\int_{-1}^{+1}N_I'(\xi).\frac{L_e}{2}d\xi)\Big]-\Big[n_e.(\sum_{I=1}^{n=3}\delta u_I.\int_{-1}^{+1}N_I(\xi).\frac{L_e}{2}d\xi)+\\
&q_e.(\sum_{I=1}^{n=3}\delta w_I.\int_{-1}^{+1}N_I(\xi).\frac{L_e}{2}d\xi)+\underbrace{m_e}_{=0}.(\sum_{I=1}^{n=3}\delta\psi_I.\int_{-1}^{+1}N_I(\xi).\frac{L_e}{2}d\xi)\Big]\Big]=0
\end{aligned}
\tag{2.32}
$$

Mathematically there is no way to integrate the terms analytically. Thus, Gauss quadrature is applied ($n_p$ is the number of Gauss points).

$$
\begin{aligned}
G(u,\eta) \approx \bigcup_{j=1}^{n_e} \Big[ \Big[ & N_e.(\sum_{I=1}^{n=3} \delta u_I. \sum_{p=1}^{n_p} (N_I'(\xi_p).\cos\psi_e.\frac{L_e}{2}.W_p) + \sum_{I=1}^{n=3} \delta w_I. \sum_{p=1}^{n_p} (N_I'(\xi_p).\sin\psi_e.\frac{L_e}{2}.W_p) + \\
& \sum_{I=1}^{n=3} \delta\psi_I. \sum_{p=1}^{n_p} (N_I(\xi_p).\alpha_e.\frac{L_e}{2}.W_p)) + Q_e.(\sum_{I=1}^{n=3} \delta w_I. \sum_{p=1}^{n_p} (N_I'(\xi_p).\cos\psi_e.\frac{L_e}{2}.W_p) - \\
& \sum_{I=1}^{n=3} \delta u_I. \sum_{p=1}^{n_p} (N_I'(\xi_p).\sin\psi_e.\frac{L_e}{2}.W_p) + \sum_{I=1}^{n=3} \delta\psi_I. \sum_{p=1}^{n_p} (N_I(\xi_p).\beta_e.\frac{L_e}{2}.W_p)) + \\
& M_e.(\sum_{I=1}^{n=3} \delta\psi_I. \sum_{p=1}^{n_p} N_I'(\xi_p).\frac{L_e}{2}.W_p) \Big] - \Big[ n_e.(\sum_{I=1}^{n=3} \delta u_I. \sum_{p=1}^{n_p} N_I(\xi_p).\frac{L_e}{2}.W_p) + \\
& q_e.(\sum_{I=1}^{n=3} \delta w_I. \sum_{p=1}^{n_p} N_I(\xi_p).\frac{L_e}{2}.W_p) + \underbrace{m_e}_{=0}.(\sum_{I=1}^{n=3} \delta\psi_I. \sum_{p=1}^{n_p} N_I(\xi_p).\frac{L_e}{2}.W_p) \Big] \Big] \approx 0
\end{aligned}
\tag{2.33}
$$

then $\frac{L_e}{2}$ drawn out.

$$
\begin{aligned}
G(u,\eta) \approx \bigcup_{j=1}^{n_e} \Big[ \frac{L_e}{2}. \Big[ & N_e.(\sum_{I=1}^{n=3} \delta u_I. \sum_{p=1}^{n_p} (N_I'(\xi_p).\cos\psi_e.W_p) + \sum_{I=1}^{n=3} \delta w_I. \sum_{p=1}^{n_p} (N_I'(\xi_p).\sin\psi_e.W_p) + \\
& \sum_{I=1}^{n=3} \delta\psi_I. \sum_{p=1}^{n_p} (N_I(\xi_p).\alpha_e.W_p)) + Q_e.(\sum_{I=1}^{n=3} \delta w_I. \sum_{p=1}^{n_p} (N_I'(\xi_p).\cos\psi_e.W_p) - \\
& \sum_{I=1}^{n=3} \delta u_I. \sum_{p=1}^{n_p} (N_I'(\xi_p).\sin\psi_e.W_p) + \sum_{I=1}^{n=3} \delta\psi_I. \sum_{p=1}^{n_p} (N_I(\xi_p).\beta_e.W_p)) + \\
& M_e.(\sum_{I=1}^{n=3} \delta\psi_I. \sum_{p=1}^{n_p} N_I'(\xi_p).W_p) \Big] - \Big[ n_e.(\sum_{I=1}^{n=3} \delta u_I. \sum_{p=1}^{n_p} N_I(\xi_p).W_p) + \\
& q_e.(\sum_{I=1}^{n=3} \delta w_I. \sum_{p=1}^{n_p} N_I(\xi_p).W_p) + \underbrace{m_e}_{=0}.(\sum_{I=1}^{n=3} \delta\psi_I. \sum_{p=1}^{n_p} N_I(\xi_p).W_p) \Big] \Big] \approx 0
\end{aligned}
\tag{2.34}
$$

$$
\begin{aligned}
G(u,\eta) \approx \bigcup_{j=1}^{n_e} \Bigg[ \frac{L_e}{2}. \Big[ & \left[ \sum_{I=1}^{n=3} \delta u_I \quad \sum_{I=1}^{n=3} \delta w_I \quad \sum_{I=1}^{n=3} \delta \psi_I \right] . \begin{bmatrix} \sum_{p=1}^{n_p} N_I'(\xi_p).\cos\psi_e.W_p \\ \sum_{p=1}^{n_p} N_I'(\xi_p).\sin\psi_e.W_p \\ \sum_{p=1}^{n_p} N_I(\xi_p).\alpha_e.W_p \end{bmatrix} .N_e + \\
& \left[ \sum_{I=1}^{n=3} \delta u_I \quad \sum_{I=1}^{n=3} \delta w_I \quad \sum_{I=1}^{n=3} \delta \psi_I \right] . \begin{bmatrix} \sum_{p=1}^{n_p} -N_I'(\xi_p).\sin\psi_e.W_p \\ \sum_{p=1}^{n_p} N_I'(\xi_p).\cos\psi_e.W_p \\ \sum_{p=1}^{n_p} N_I(\xi_p).\beta_e.W_p \end{bmatrix} .Q_e + \\
& \left[ \sum_{I=1}^{n=3} \delta u_I \quad \sum_{I=1}^{n=3} \delta w_I \quad \sum_{I=1}^{n=3} \delta \psi_I \right] . \begin{bmatrix} 0 \\ 0 \\ \sum_{p=1}^{n_p} N_I'(\xi_p).W_p \end{bmatrix} .M_e \Big] - \Big[ \\
& \left[ \sum_{I=1}^{n=3} \delta u_I \quad \sum_{I=1}^{n=3} \delta w_I \quad \sum_{I=1}^{n=3} \delta \psi_I \right] . \begin{bmatrix} \sum_{p=1}^{n_p} N_I(\xi_p).W_p \\ 0 \\ 0 \end{bmatrix} .n_e + \\
& \left[ \sum_{I=1}^{n=3} \delta u_I \quad \sum_{I=1}^{n=3} \delta w_I \quad \sum_{I=1}^{n=3} \delta \psi_I \right] . \begin{bmatrix} 0 \\ \sum_{p=1}^{n_p} N_I(\xi_p).W_p \\ 0 \end{bmatrix} .q_e + \\
& \left[ \sum_{I=1}^{n=3} \delta u_I \quad \sum_{I=1}^{n=3} \delta w_I \quad \sum_{I=1}^{n=3} \delta \psi_I \right] . \begin{bmatrix} 0 \\ 0 \\ \sum_{p=1}^{n_p} N_I(\xi_p).W_p \end{bmatrix} . \underbrace{m_e}_{=0} \Big] \Bigg] \approx 0
\end{aligned}
\tag{2.35}
$$

and then arrange it in matrix form

$$G(u,\eta) \approx \bigcup_{j=1}^{n_e} \Bigg[ \frac{L_e}{2} . \Big[ \begin{bmatrix} \sum_{I=1}^{n=3} \delta u_I & \sum_{I=1}^{n=3} \delta w_I & \sum_{I=1}^{n=3} \delta \psi_I \end{bmatrix} . \\ \begin{bmatrix} \sum_{p=1}^{n_p} N_I'(\xi_p).\cos\psi_e.W_p & \sum_{p=1}^{n_p} -N_I'(\xi_p).\sin\psi_e.W_p & 0 \\ \sum_{p=1}^{n_p} N_I'(\xi_p).\sin\psi_e.W_p & \sum_{p=1}^{n_p} N_I'(\xi_p).\cos\psi_e.W_p & 0 \\ \sum_{p=1}^{n_p} N_I(\xi_p).\alpha_e.W_p & \sum_{p=1}^{n_p} N_I(\xi_p).\beta_e.W_p & \sum_{p=1}^{n_p} N_I'(\xi_p).W_p \end{bmatrix} . \begin{bmatrix} N_e \\ Q_e \\ M_e \end{bmatrix} \Big] - \\ \Big[ \begin{bmatrix} \sum_{I=1}^{n=3} \delta u_I & \sum_{I=1}^{n=3} \delta w_I & \sum_{I=1}^{n=3} \delta \psi_I \end{bmatrix} . \begin{bmatrix} \sum_{p=1}^{n_p} N_I(\xi_p).W_p & 0 & 0 \\ 0 & \sum_{p=1}^{n_p} N_I(\xi_p).W_p & 0 \\ 0 & 0 & \sum_{p=1}^{n_p} N_I(\xi_p).W_p \end{bmatrix} . \\ \begin{bmatrix} n_e \\ q_e \\ 0 \end{bmatrix} \Big] \Bigg] \approx 0 \tag{2.36}$$

therefore

$$G(u,\eta) \approx \bigcup_{j=1}^{n_e} \Bigg[ \frac{L_e}{2} . \sum_{I=1}^{n=3} \begin{bmatrix} \delta u_I & \delta w_I & \delta \psi_I \end{bmatrix} . \Big[ \sum_{p=1}^{n_p} W_p . \begin{bmatrix} N_I'(\xi_p).\cos\psi_e & -N_I'(\xi_p).\sin\psi_e & 0 \\ N_I'(\xi_p).\sin\psi_e & N_I'(\xi_p).\cos\psi_e & 0 \\ N_I(\xi_p).\alpha_e & N_I(\xi_p).\beta_e & N_I'(\xi_p) \end{bmatrix} . \\ \begin{bmatrix} N_e \\ Q_e \\ M_e \end{bmatrix} - \sum_{p=1}^{n_p} W_p . \begin{bmatrix} N_I(\xi_p) & 0 & 0 \\ 0 & N_I(\xi_p) & 0 \\ 0 & 0 & N_I(\xi_p) \end{bmatrix} . \begin{bmatrix} n_e \\ q_e \\ 0 \end{bmatrix} \Big] \Bigg] \approx 0 \tag{2.37}$$

$$G(u,\eta) \approx \bigcup_{j=1}^{n_e} \Big[ \frac{L_e}{2} . \sum_{I=1}^{n=3} \boldsymbol{\eta}_I^T . \big[ \sum_{p=1}^{n_p} W_p . \boldsymbol{B}_I^T(\xi_p, \boldsymbol{u}_I) . \boldsymbol{S}_e(\xi_p, \boldsymbol{u}_I) - \sum_{p=1}^{n_p} W_p . \boldsymbol{N}_I(\xi_p) . \boldsymbol{q}_e \big] \Big] \approx 0$$

(2.38)

$$\boxed{G(u,\eta) \approx \bigcup_{j=1}^{n_e} \left[ \frac{L_e}{2} . \sum_{I=1}^{n=3} \boldsymbol{\eta}_I^T . \sum_{p=1}^{n_p} W_p . \Big[ \boldsymbol{B}_I^T(\xi_p, \boldsymbol{u}_I) . \boldsymbol{S}_e(\xi_p, \boldsymbol{u}_I) - \boldsymbol{N}_I(\xi_p) . \boldsymbol{q}_e \Big] \right] \approx 0} \tag{2.39}$$

The symbol $\bigcup$ in equations describes the assembly of all elements including the enforcement of continuity for the displacements and rotations along the element boundaries. $L_e$ is the length of one finite element. Note that the integrals in (2.32) cannot be computed analytically in general. Thus Gauss quadrature is applied. By transforming the integral to the local finite element coordinate $\xi_p$ the relation does not depend on $X_1$ coordination. For a linear two-node element, one-point integration is sufficient to exactly integrate the bending part. In that case, the shear term is under integrated. The latter, however, is advantageous since it avoids shear locking. This effect is well known from the linear theory and will not be studied in detail. For a quadratic element with three nodal points, two Gauss points for the integration have to be selected.
From equation (2.39) we can realize that the Residual vector $\boldsymbol{R}_I$ can be expressed like

$$\boxed{\boldsymbol{R}_I(\boldsymbol{u}_I) = \bigcup_{j=1}^{n_e} \left[ \frac{L_e}{2} . \sum_{I=1}^{n=3} \sum_{p=1}^{n_p} W_p . \boldsymbol{B}_I^T(\xi_p, \boldsymbol{u}_I) . \boldsymbol{S}_e(\xi_p, \boldsymbol{u}_I) \right]} \tag{2.40}$$

# 2.6 Discretization of the Linearization of the Weak Form

Based on the linearization of (2.39), the Newton or the arc-length method can be applied to solve (2.39). Within this linearization process, it is essential that no terms are neglected in order to obtain the quadratic convergence properties of Newton method. The complete linearization of the weak form (2.3) can be derived once a constitutive equation is selected. Here (2.8) is used and the linearization of $G$ is a formal procedure and it yields

$$\begin{aligned} DG(\boldsymbol{u},\boldsymbol{\eta}).\Delta\boldsymbol{u} = & \int_0^l (\delta\epsilon.EA.\Delta\epsilon + \delta\gamma.G\hat{A}.\Delta\gamma + \delta\kappa.EI.\Delta\kappa)dx + \\ & + \int_0^l (\Delta\delta\epsilon.N + \Delta\delta\gamma.Q + \Delta\delta\kappa.M)dx. \end{aligned} \tag{2.41}$$

Since the mathematical rules which are applied to compute variations and linearization do not differ the variation $\delta\epsilon$ and linearization $\Delta\epsilon$ of the strains have the same structure.

## 2.6.1 Variation of Strain $\Delta\epsilon$

The variation of strain vector $\Delta\boldsymbol{\epsilon}$ can be written

$$\begin{aligned} \Delta\epsilon &= \Delta u'.\cos\psi - (1+u').\Delta\psi.\sin\psi + \Delta w'.\sin\psi + w'.\Delta\psi.\cos\psi \\ \Delta\gamma &= \Delta w'.\cos\psi - w'.\Delta\psi.\sin\psi - \Delta u'.\sin\psi - (1+u').\Delta\psi.\cos\psi \\ \Delta\kappa &= \Delta\psi' \end{aligned} \tag{2.42}$$

and the matrix form is

$$\boxed{\begin{aligned} &\Delta\boldsymbol{\epsilon} = \boldsymbol{T}(\psi).\Delta\boldsymbol{u}' + \frac{\partial \boldsymbol{T}(\psi)}{\partial\psi}.\boldsymbol{u}'.\Delta\psi - \frac{\partial \boldsymbol{\Psi}(\psi)}{\partial\psi}.\Delta\psi \\ &\Delta\boldsymbol{u}' = \begin{bmatrix}\Delta u' & \Delta w' & \Delta\psi'\end{bmatrix}^T \end{aligned}} \tag{2.43}$$

## 2.6.2 Variation of Strain for one Element $\Delta\boldsymbol{\epsilon}_e$

The variation of strain vector of an element $\Delta\boldsymbol{\epsilon}_e$ with shape functions can be interpolated

$$\begin{bmatrix}\Delta\epsilon_e \\ \Delta\gamma_e \\ \Delta\kappa_e\end{bmatrix} = \sum_{K=1}^{n=3} \begin{bmatrix} N'_K(X_1).\cos\psi_e & N'_K(X_1).\sin\psi_e & N_K(X_1).\alpha_e \\ -N'_K(X_1).\sin\psi_e & N'_K(X_1).\cos\psi_e & N_K(X_1).\beta_e \\ 0 & 0 & N'_K(X_1)\end{bmatrix} \cdot \begin{bmatrix}\Delta u_K \\ \Delta w_K \\ \Delta\psi_K\end{bmatrix} \tag{2.44}$$

and the matrix form is

$$\boxed{\begin{aligned} &\Delta\boldsymbol{\epsilon}_e = \sum_{K=1}^{n=3}[\boldsymbol{B}_K.\Delta\boldsymbol{u}_K] \\ &\boldsymbol{B}_K(X_1) = \begin{bmatrix} N'_K(X_1).\cos\psi_e & N'_K(X_1).\sin\psi_e & N_K(X_1).\alpha_e \\ -N'_K(X_1).\sin\psi_e & N'_K(X_1).\cos\psi_e & N_K(X_1).\beta_e \\ 0 & 0 & N'_K(X_1)\end{bmatrix} \end{aligned}} \tag{2.45}$$

## 2.6.3 Variation of Displacement $\Delta\boldsymbol{u}_e$

The variation of displacement vector of an element $\Delta\boldsymbol{u}_e$ with shape functions can be written

$$\begin{aligned} \Delta u_e &= \sum_{K=1}^{n=3} N_K(X_1).\Delta u_K = N_1(X_1).\Delta u_1 + N_2(X_1).\Delta u_2 + N_3(X_1).\Delta u_3 \\ \Delta w_e &= \sum_{K=1}^{n=3} N_K(X_1).\Delta w_K = N_1(X_1).\Delta w_1 + N_2(X_1).\Delta w_2 + N_3(X_1).\Delta w_3 \\ \Delta\psi_e &= \sum_{K=1}^{n=3} N_K(X_1).\Delta\psi_K = N_1(X_1).\Delta\psi_1 + N_2(X_1).\Delta\psi_2 + N_3(X_1).\Delta\psi_3 \end{aligned} \tag{2.46}$$

and the matrix form is

$$\boxed{\begin{aligned}&\Delta \boldsymbol{u}_e = \sum_{K=1}^{n=3} [\boldsymbol{N}_K . \Delta \boldsymbol{u}_K] \\ &\begin{bmatrix} \Delta u_e \\ \Delta w_e \\ \Delta \psi_e \end{bmatrix} = \sum_{K=1}^{n=3} \begin{bmatrix} N_K(X_1) & 0 & 0 \\ 0 & N_K(X_1) & 0 \\ 0 & 0 & N_K(X_1) \end{bmatrix} \cdot \begin{bmatrix} \Delta u_K \\ \Delta w_K \\ \Delta \psi_K \end{bmatrix}\end{aligned}} \tag{2.47}$$

### 2.6.4 Variation of Derivation of Displacement $\Delta \boldsymbol{u}_e'$

The variation of derivation of displacement of an element $\Delta \boldsymbol{u}_e'$ with shape functions can be interpolated

$$\begin{aligned}
\Delta u_e' &= \sum_{K=1}^{n=3} N_K'(X_1).\Delta u_K = N_1'(X_1).\Delta u_1 + N_2'(X_1).\Delta u_2 + N_3'(X_1).\Delta u_3 \\
\Delta w_e' &= \sum_{K=1}^{n=3} N_K'(X_1).\Delta w_K = N_1'(X_1).\Delta w_1 + N_2'(X_1).\Delta w_2 + N_3'(X_1).\Delta w_3 \\
\Delta \psi_e' &= \sum_{K=1}^{n=3} N_K'(X_1).\Delta \psi_K = N_1'(X_1).\Delta \psi_1 + N_2'(X_1).\Delta \psi_2 + N_3'(X_1).\Delta \psi_3
\end{aligned} \tag{2.48}$$

and the matrix form is

$$\boxed{\begin{aligned}&\Delta \boldsymbol{u}_e' = \sum_{K=1}^{n=3} [\boldsymbol{N}_K' . \Delta \boldsymbol{u}_K] \\ &\begin{bmatrix} \Delta u_e' \\ \Delta w_e' \\ \Delta \psi_e' \end{bmatrix} = \sum_{K=1}^{n=3} \begin{bmatrix} N_K'(X_1) & 0 & 0 \\ 0 & N_K'(X_1) & 0 \\ 0 & 0 & N_K'(X_1) \end{bmatrix} \cdot \begin{bmatrix} \Delta u_K \\ \Delta w_K \\ \Delta \psi_K \end{bmatrix}\end{aligned}} \tag{2.49}$$

### 2.6.5 Variation of Virtual Axial Strain $\Delta\delta\boldsymbol{\epsilon}_e$

The variation of virtual axial strain of an element with shape functions can be written

$$\begin{aligned}
\Delta\delta\epsilon_e = {} & [-\delta u_e'.\sin\psi_e + \delta w_e'.\cos\psi_e].\Delta\psi_e + [-\Delta u_e'.\sin\psi_e + \Delta w_e'.\cos\psi_e].\delta\psi_e + \\
& + \delta\psi_e.[-(1+u_e').\cos\psi_e - w_e'.\sin\psi_e].\Delta\psi_e
\end{aligned} \tag{2.50}$$

$$\begin{aligned}\Delta\delta\epsilon_e = &[(-\sum_{I=1}^{n=3} N_I'(X_1).\delta u_I).\sin\psi_e + (\sum_{I=1}^{n=3} N_I'(X_1).\delta w_I).\cos\psi_e].(\sum_{K=1}^{n=3} N_K(X_1).\Delta\psi_K)+\\ &+[(-\sum_{K=1}^{n=3} N_K'(X_1).\Delta u_K).\sin\psi_e + (\sum_{K=1}^{n=3} N_K'(X_1).\Delta w_K).\cos\psi_e].(\sum_{I=1}^{n=3} N_I(X_1).\delta\psi_I)+\\ &+(\sum_{I=1}^{n=3} N_I(X_1).\delta\psi_I).\underbrace{[-(1+u_e').\cos\psi_e - w_e'.\sin\psi_e]}_{\alpha_3}.(\sum_{K=1}^{n=3} N_K(X_1).\Delta\psi_K)\end{aligned} \tag{2.51}$$

$$\begin{aligned}\Delta\delta\epsilon_e = &\sum_{I=1}^{n=3}\sum_{K=1}^{n=3} \delta u_I.[-N_I'(X_1).N_K(X_1).\sin\psi_e].\Delta\psi_K + \delta w_I.[N_I'(X_1).N_K(X_1).\cos\psi_e].\Delta\psi_K+\\ &+\delta\psi_I.[-N_I(X_1).N_K'(X_1).\sin\psi_e].\Delta u_K + \delta\psi_I.[N_I(X_1).N_K'(X_1).\cos\psi_e].\Delta w_K+\\ &+\delta\psi_I.[\alpha_3.N_I(X_1).N_K(X_1)].\Delta\psi_K\end{aligned} \tag{2.52}$$

and the matrix format for variation of virtual axial strain is

$$\boxed{\begin{aligned}&\Delta\delta\epsilon_e = \sum_{I=1}^{n=3}\sum_{K=1}^{n=3}\begin{bmatrix}\delta u_I & \delta w_I & \delta\psi_I\end{bmatrix}.\\ &\begin{bmatrix} 0 & 0 & -N_I'(X_1).N_K(X_1).\sin\psi_e \\ 0 & 0 & N_I'(X_1).N_K(X_1).\cos\psi_e \\ -N_I(X_1).N_K'(X_1).\sin\psi_e & N_I(X_1).N_K'(X_1).\cos\psi_e & \alpha_3.N_I(X_1).N_K(X_1)\end{bmatrix}.\begin{bmatrix}\Delta u_K \\ \Delta w_K \\ \Delta\psi_K\end{bmatrix}\end{aligned}} \tag{2.53}$$

$$\boxed{\Delta\delta\epsilon_e = \sum_{I=1}^{n=3}\sum_{K=1}^{n=3} \boldsymbol{\eta}_I^T.\boldsymbol{G}_{IK}^N(X_1).\Delta\boldsymbol{u}_K} \tag{2.54}$$

### 2.6.6 Variation of Virtual Shear Strain $\Delta\delta\gamma_e$

The variation of virtual shear strain of an element with shape functions can be written

$$\begin{aligned}\Delta\delta\gamma_e = &[-\delta u_e'.\cos\psi_e - \delta w_e'.\sin\psi_e].\Delta\psi_e + [-\Delta u_e'.\cos\psi_e - \Delta w_e'.\sin\psi_e].\delta\psi_e+\\ &+\delta\psi_e.[(1+u_e').\sin\psi_e - w_e'.\cos\psi_e].\Delta\psi_e\end{aligned} \tag{2.55}$$

$$\begin{aligned}\Delta\delta\gamma_e = &[(-\sum_{I=1}^{n=3} N_I'(X_1).\delta u_I).\cos\psi_e - (\sum_{I=1}^{n=3} N_I'(X_1).\delta w_I).\sin\psi_e].(\sum_{K=1}^{n=3} N_K(X_1).\Delta\psi_K)+ \\ &+ [(-\sum_{K=1}^{n=3} N_K'(X_1).\Delta u_K).\cos\psi_e - (\sum_{K=1}^{n=3} N_K'(X_1).\Delta w_K).\sin\psi_e].(\sum_{I=1}^{n=3} N_I(X_1).\delta\psi_I)+ \\ &+ (\sum_{I=1}^{n=3} N_I(X_1).\delta\psi_I).\underbrace{[(1+u_e').\sin\psi_e - w_e'.\cos\psi_e]}_{\alpha_4}.(\sum_{K=1}^{n=3} N_K(X_1).\Delta\psi_K)\end{aligned} \tag{2.56}$$

$$\begin{aligned}\Delta\delta\gamma_e = &\sum_{I=1}^{n=3}\sum_{K=1}^{n=3} \delta u_I.[-N_I'(X_1).N_K(X_1).\cos\psi_e].\Delta\psi_K + \delta w_I.[-N_I'(X_1).N_K(X_1).\sin\psi_e].\Delta\psi_K+ \\ &+ \delta\psi_I.[-N_I(X_1).N_K'(X_1).\cos\psi_e].\Delta u_K + \delta\psi_I.[-N_I(X_1).N_K'(X_1).\sin\psi_e].\Delta w_K+ \\ &+ \delta\psi_I.[\alpha_4.N_I(X_1).N_K(X_1)].\Delta\psi_K\end{aligned} \tag{2.57}$$

and the matrix format for variation of virtual shear strain is

$$\boxed{\begin{aligned}&\Delta\delta\gamma_e = \sum_{I=1}^{n=3}\sum_{K=1}^{n=3} \begin{bmatrix}\delta u_I & \delta w_I & \delta\psi_I\end{bmatrix}. \\ &\begin{bmatrix} 0 & 0 & -N_I'(X_1).N_K(X_1).\cos\psi_e \\ 0 & 0 & -N_I'(X_1).N_K(X_1).\sin\psi_e \\ -N_I(X_1).N_K'(X_1).\cos\psi_e & -N_I(X_1).N_K'(X_1).\sin\psi_e & \alpha_4.N_I(X_1).N_K(X_1)\end{bmatrix} . \begin{bmatrix}\Delta u_K \\ \Delta w_K \\ \Delta\psi_K\end{bmatrix}\end{aligned}} \tag{2.58}$$

$$\boxed{\Delta\delta\gamma_e = \sum_{I=1}^{n=3}\sum_{K=1}^{n=3} \boldsymbol{\eta}_I^T.\boldsymbol{G}_{IK}^Q(X_1).\Delta\boldsymbol{u}_K} \tag{2.59}$$

### 2.6.7 Variation of Virtual Curvature $\Delta\delta\boldsymbol{\kappa}_e$

$$\boxed{\Delta\delta\kappa_e = 0} \tag{2.60}$$

### 2.6.8 Tangent Matrix

The tangent stiffness matrix $\boldsymbol{K}^{tangent}$ is formulated based on the linearization (2.41) which can be expressed discretely

$$DG(\boldsymbol{u},\boldsymbol{\eta}).\Delta\boldsymbol{u} = \bigcup_{j=1}^{n_e}\left[\int_0^{L_e}(\delta\boldsymbol{\epsilon}_e^T.\boldsymbol{D}.\Delta\boldsymbol{\epsilon}_e)dx + \int_0^{L_e}(\Delta\delta\epsilon_e.N_e + \Delta\delta\gamma_e.Q_e)dx\right] \tag{2.61}$$

$$DG(\boldsymbol{u},\boldsymbol{\eta}).\Delta\boldsymbol{u} = \bigcup_{j=1}^{n_e}\Big[\int_0^{L_e}\Big[(\sum_{I=1}^{n=3}\boldsymbol{\eta}_I^T.\boldsymbol{B}_I^T(X_1)).\boldsymbol{D}.(\sum_{K=1}^{n=3}\boldsymbol{B}_K(X_1).\Delta\boldsymbol{u}_K)\Big]dX_1+$$
$$\int_0^{L_e}\Big[N_e(X_1).(\sum_{I=1}^{n=3}\sum_{K=1}^{n=3}\boldsymbol{\eta}_I^T.\boldsymbol{G}_{IK}^N(X_1).\Delta\boldsymbol{u}_K)+Q_e(X_1).(\sum_{I=1}^{n=3}\sum_{K=1}^{n=3}\boldsymbol{\eta}_I^T.\boldsymbol{G}_{IK}^Q(X_1).\Delta\boldsymbol{u}_K)\Big]dX_1\Big] \tag{2.62}$$

Based on constitutive equations it can be realize that

$$N_e(X_1) = EA.\epsilon_e(X_1), \quad N_e(X_1) = EA.[\sum_{I=1}^{n=3}N_I'(X_1).u_I.\cos\psi_e+\sum_{I=1}^{n=3}N_I'(X_1).w_I.\sin\psi_e-1+\cos\psi_e]$$
$$Q_e(X_1) = G\hat{A}.\gamma_e(X_1), \quad Q_e(X_1) = G\hat{A}.[\sum_{I=1}^{n=3}N_I'(X_1).w_I.\cos\psi_e-\sum_{I=1}^{n=3}N_I'(X_1).u_I.\sin\psi_e-\sin\psi_e] \tag{2.63}$$

Therefore equation (2.62) can be expressed

$$DG(\boldsymbol{u},\boldsymbol{\eta}).\Delta\boldsymbol{u} = \bigcup_{j=1}^{n_e}\Big[\sum_{I=1}^{n=3}\sum_{K=1}^{n=3}\boldsymbol{\eta}_I^T.\Big[\int_0^{L_e}\boldsymbol{B}_I^T(X_1).\boldsymbol{D}.\boldsymbol{B}_K(X_1)dX_1\Big].\Delta\boldsymbol{u}_K+$$
$$\sum_{I=1}^{n=3}\sum_{K=1}^{n=3}\boldsymbol{\eta}_I^T.\Big[\int_0^{L_e}N_e(X_1).\boldsymbol{G}_{IK}^N(X_1)+Q_e(X_1).\boldsymbol{G}_{IK}^Q(X_1)dX_1\Big].\Delta\boldsymbol{u}_K\Big] \tag{2.64}$$

$$DG(\boldsymbol{u},\boldsymbol{\eta}).\Delta\boldsymbol{u} = \bigcup_{j=1}^{n_e}\Big[\sum_{I=1}^{n=3}\sum_{K=1}^{n=3}\boldsymbol{\eta}_I^T.\Big[\int_0^{L_e}\boldsymbol{B}_I^T(X_1).\boldsymbol{D}.\boldsymbol{B}_K(X_1)+$$
$$N_e(X_1).\boldsymbol{G}_{IK}^N(X_1)+Q_e(X_1).\boldsymbol{G}_{IK}^Q(X_1)dX_1\Big].\Delta\boldsymbol{u}_K\Big] \tag{2.65}$$

$$\boxed{DG(\boldsymbol{u},\boldsymbol{\eta}).\Delta\boldsymbol{u} \approx \bigcup_{j=1}^{n_e}\Big[\frac{L_e}{2}.\sum_{I=1}^{n=3}\sum_{K=1}^{n=3}\boldsymbol{\eta}_I^T.\Big[\sum_{p=1}^{n_p}W_p.[\boldsymbol{B}_I^T(\xi_p).\boldsymbol{D}.\boldsymbol{B}_K(\xi_p)+ N_e(\xi_p).\boldsymbol{G}_{IK}^N(\xi_p)+Q_e(\xi_p).\boldsymbol{G}_{IK}^Q(\xi_p)]\Big].\Delta\boldsymbol{u}_K\Big]} \tag{2.66}$$

and the compact format of tangent stiffness matrix is

$$\boxed{\boldsymbol{K}_{IK}^{tangent} \approx \bigcup_{j=1}^{n_e}\Big[\frac{L_e}{2}.\sum_{I=1}^{n=3}\sum_{K=1}^{n=3}\boldsymbol{\eta}_I^T.\Big[\sum_{p=1}^{n_p}W_p.[\boldsymbol{B}_I^T(\xi_p).\boldsymbol{D}.\boldsymbol{B}_K(\xi_p)+ N_e(\xi_p).\boldsymbol{G}_{IK}^N(\xi_p)+Q_e(\xi_p).\boldsymbol{G}_{IK}^Q(\xi_p)]\Big]\Big]} \tag{2.67}$$

These equations are related to the local coordinate system of the straight beam axis. Since beam members are used in most cases within the construction of complex structures, like multi-story frames in which the beams are located in different positions, the matrices and vectors have to be transformed to a global coordinate system. This can be performed in the same way as in the linear theory since all equations are referred to the initial configuration. By such transformation, the local nodal displacements and rotations $\boldsymbol{u}_I^{local}$ at node $I$ can be expressed in terms of the global deformations $\boldsymbol{u}_I^{global}$ via

$$\boldsymbol{u}_I^{local} = \bar{\boldsymbol{T}}_I . \boldsymbol{u}_I^{global} \tag{2.68}$$

The explicit form is given in the two-dimensional case by

$$\begin{bmatrix} u_I \\ w_I \\ \psi_I \end{bmatrix}^{local} = \begin{bmatrix} \cos\alpha & \sin\alpha & 0 \\ -\sin\alpha & \cos\alpha & 0 \\ 0 & 0 & 1 \end{bmatrix} \cdot \begin{bmatrix} u_I \\ w_I \\ \psi_I \end{bmatrix}^{global} \tag{2.69}$$

The angle $\alpha$ refers to the angle between the local and global coordinate axis $X_1$. Using this transformation, the local form of (2.67) of the tangent matrix $K_{IK}^{tangent}$ can be expressed in terms of the global coordinates

$$\boldsymbol{K}_{IK}^{tangent^{global}} = \bar{\boldsymbol{T}}_I^T . \boldsymbol{K}_{IK}^{tangent^{local}} . \bar{\boldsymbol{T}}_I \tag{2.70}$$

and also

$$\boldsymbol{R}_I^{global} = \bar{\boldsymbol{T}}_I^T . \boldsymbol{R}_I^{local} \tag{2.71}$$

# Chapter 3

# The Theory Of Moderate Rotations

## 3.1 Kinematics

In this chapter the previous beam theory will be considered but with moderate rotation. In equation(2.1) there are $sin\psi$ and $\cos\psi$ ,therefore based on Taylor series at $\psi_0$ the trigonometric function can be rewritten:

$\sin(\psi_0 + \psi) = \sin\psi_0 + \cos\psi_0.\psi + \frac{1}{2}\sin\psi_0.\psi^2 + ...$

$\cos(\psi_0 + \psi) = \cos\psi_0 - \sin\psi_0.\psi - \frac{1}{2}\cos\psi_0.\psi^2 + ...$

for $\psi_0 = 0$ it follows:

$\sin(\psi) \approx \psi$

$\cos(\psi) \approx 1 - \frac{1}{2}\psi^2$

inserting above equations in equation(2.1) and including all terms up to second order yields

$$\begin{aligned}
\epsilon(X_1) &= u'(X_1) + \psi(X_1)w'(X_1) - \frac{1}{2}\psi^2(X_1),\\
\gamma(X_1) &= w'(X_1) - (1 + u'(X_1))\psi(X_1),\\
\kappa(X_1) &= \psi'(X_1)
\end{aligned} \tag{3.1}$$

The strain can also be formulated in matrix notation

$$\begin{aligned}
&\boldsymbol{\epsilon}(X_1) = \bar{\boldsymbol{T}}(\psi).\boldsymbol{u}'(X_1) - \bar{\boldsymbol{\Psi}}\\
&\boldsymbol{\epsilon} = \begin{bmatrix}\epsilon\\ \gamma\\ \kappa\end{bmatrix}, \bar{\boldsymbol{T}} = \begin{bmatrix}1 & \psi & 0\\ -\psi & 1 & 0\\ 0 & 0 & 1\end{bmatrix}, \boldsymbol{u}' = \begin{bmatrix}u'\\ w'\\ \psi'\end{bmatrix}, \bar{\boldsymbol{\Psi}} = \begin{bmatrix}\frac{1}{2}\psi^2\\ \psi\\ 0\end{bmatrix}
\end{aligned} \tag{3.2}$$

The approximation (3.2) contains all quadratic terms. The strain measures are not much simpler than the exact ones provided in (2.2); only the trigonometric functions of the angle $\psi$ disappear.

## 3.2 Weak Form of Equilibrium

For theory of moderate rotation, the variation of strains yields

$$\begin{aligned} \delta\epsilon &= \delta u' + \delta w'.\psi + \delta\psi.w' - \psi.\delta\psi \\ \delta\gamma &= \delta w' - \delta u'.\psi - (1+u').\delta\psi \\ \delta\kappa &= \delta\psi' \end{aligned} \tag{3.3}$$

and in Matrix form it can be written

$$\begin{aligned} \delta\boldsymbol{\epsilon}(X_1) &= \bar{\boldsymbol{T}}(\psi).\boldsymbol{\eta}'(X_1) + [\frac{\partial\bar{\boldsymbol{T}}(\psi)}{\partial\psi}.\boldsymbol{u}'(X_1) - \frac{\partial\bar{\boldsymbol{\Psi}}(\psi)}{\partial\psi}].\delta\psi \\ \boldsymbol{\eta}' = \begin{bmatrix} \delta u' \\ \delta w' \\ \delta\psi' \end{bmatrix} &, \frac{\partial\bar{\boldsymbol{T}}(\psi)}{\partial\psi} = \begin{bmatrix} 0 & 1 & 0 \\ -1 & 0 & 0 \\ 0 & 0 & 0 \end{bmatrix}, \frac{\partial\bar{\boldsymbol{\Psi}}(\psi)}{\partial\psi} = \begin{bmatrix} \psi \\ 1 \\ 0 \end{bmatrix} \end{aligned} \tag{3.4}$$

By inserting this relation in the weak form (2.4), the first term can be specified as

$$\int_0^l \delta\boldsymbol{\epsilon}^T(X_1).\boldsymbol{S}dx = \int_0^l \left[\boldsymbol{\eta}'^T(X_1).\bar{\boldsymbol{T}}^T(\psi) + \delta\psi.\boldsymbol{u}'^T(X_1).(\frac{\partial\bar{\boldsymbol{T}}(\psi)}{\partial\psi})^T - \delta\psi.(\frac{\partial\bar{\boldsymbol{\Psi}}(\psi)}{\partial\psi})^T\right].\boldsymbol{S}dx \tag{3.5}$$

## 3.3 Finite Element Formulation

In an analogous way, the discrete form of the moderate rotation for nonlinear beam theories can be derived. Hence polynomials (2.9) or (2.10) can be applied as finite element interpolations for the axial displacements $u$, the deflection $w$ and the rotation. Therefore $\boldsymbol{u}_e$, $\boldsymbol{u}'_e$, $\delta\boldsymbol{u}_e$ and $\delta\boldsymbol{u}'_e$ are the same like previous chapter. In this case but $\boldsymbol{\epsilon}_e$ and $\delta\boldsymbol{\epsilon}_e$ will be calculated.

### 3.3.1 Strain $\boldsymbol{\epsilon}_e$

The strain vector of an element $\boldsymbol{\epsilon}_e$ with shape function can be interpolated

$$\begin{aligned}
\epsilon_e &= \sum_{I=1}^{n=3} N_I'(X_1).u_I + \psi_e.\sum_{I=1}^{n=3} N_I'(X_1).w_I - \frac{1}{2}.\psi_e.\sum_{I=1}^{n=3} N_I(X_1).\psi_I,\\
\gamma_e &= \sum_{I=1}^{n=3} N_I'(X_1).w_I - (1+u_e').\sum_{I=1}^{n=3} N_I(X_1).\psi_I,\\
\kappa_e &= \sum_{I=1}^{n=3} N_I'(X_1).\psi_I
\end{aligned} \tag{3.6}$$

and the matrix form can be derived

$$\begin{bmatrix}\epsilon_e\\ \gamma_e\\ \kappa_e\end{bmatrix} = \sum_{I=1}^{n=3}\Big[\begin{bmatrix} N_I'(X_1) & N_I'(X_1)\psi_e & -\frac{1}{2}\psi_e N_I\\ 0 & N_I'(X_1) & -(1+u_e')N_I(X_1)\\ 0 & 0 & N_I'(X_1)\end{bmatrix}\cdot\begin{bmatrix}u_I\\ w_I\\ \psi_I\end{bmatrix}\Big] \tag{3.7}$$

$$\boxed{\begin{aligned}
\boldsymbol{\epsilon}_e &= \sum_{I=1}^{n=3} \boldsymbol{N}_I^S.\boldsymbol{u}_I\\
\boldsymbol{N}_I^S(X_1) &= \begin{bmatrix} N_I'(X_1) & N_I'(X_1)\psi_e & -\frac{1}{2}\psi_e N_I\\ 0 & N_I'(X_1) & -(1+u_e')N_I(X_1)\\ 0 & 0 & N_I'(X_1)\end{bmatrix}
\end{aligned}} \tag{3.8}$$

$u_e$ and $\psi_e$ can be calculated with equations $(2.12)^1$ and $(2.12)^3$ respectively.

### 3.3.2 Virtual Strain $\delta\boldsymbol{\epsilon}_e$

The virtual strain vector of an element $\delta\boldsymbol{\epsilon}_e$ with shape function can be interpolated

$$\delta\epsilon_e = \sum_{I=1}^{n=3} N_I'(X_1).\delta u_I + \psi_e.\sum_{I=1}^{n=3} N_I'(X_1).\delta w_I + (w_e' - \psi_e).\sum_{I=1}^{n=3} N_I(X_1).\delta\psi_I \tag{3.9}$$

$$\delta\gamma_e = -\psi_e.\sum_{I=1}^{n=3} N_I'(X_1).\delta u_I + \sum_{I=1}^{n=3} N_I'(X_1).\delta w_I - (1+u_e').\sum_{I=1}^{n=3} N_I(X_1).\delta\psi_I \tag{3.10}$$

$$\delta\kappa_e = \sum_{I=1}^{n=3} N_I'(X_1).\delta\psi_I \tag{3.11}$$

and the matrix form is

$$\begin{bmatrix} \delta\epsilon_e \\ \delta\gamma_e \\ \delta\kappa_e \end{bmatrix} = \sum_{I=1}^{n=3} \begin{bmatrix} N'_I(X_1) & N'_I(X_1).\psi_e & (w'_e-\psi_e).N_I(X_1) \\ -N'_I(X_1).\psi_e & N'_I(X_1) & -(1+u'_e).N_I(X_1) \\ 0 & 0 & N'_I(X_1) \end{bmatrix} \cdot \begin{bmatrix} \delta u_I \\ \delta w_I \\ \delta\psi_I \end{bmatrix} \tag{3.12}$$

$$\boxed{\begin{aligned} \delta\boldsymbol{\epsilon}_e &= \sum_{I=1}^{n=3}[\boldsymbol{B}_I^S.\boldsymbol{\eta}_I] \\ \boldsymbol{B}_I^S(X_1) &= \begin{bmatrix} N'_I(X_1) & N'_I(X_1).\psi_e & (w'_e-\psi_e).N_I(X_1) \\ -N'_I(X_1).\psi_e & N'_I(X_1) & -(1+u'_e).N_I(X_1) \\ 0 & 0 & N'_I(X_1) \end{bmatrix} \end{aligned}} \tag{3.13}$$

## 3.4 Weak Form in terms of Nodal Quantities $\boldsymbol{u}_I$

By inserting the equation (3.13) in the stress divergence term, the weak form (3.5) can be completely expressed by the displacements and rotations after inserting the constitutive equation (2.8)

$$\triangleright G(u,\eta) = \bigcup_{j=1}^{n_e}\Big[\int_0^{L_e}(N.\delta\epsilon_e + Q.\delta\gamma_e + M.\delta\kappa_e)dx - \int_0^{L_e}(n.\delta u_e + q.\delta w_e)dx\Big] = 0$$

$$\begin{aligned} G(u,\eta) = \bigcup_{j=1}^{n_e}\Big[\int_0^{L_e}\Big[& N_e.(\sum_{I=1}^{n=3}N'_I(X_1).\delta u_I + \psi_e.\sum_{I=1}^{n=3}N'_I(X_1).\delta w_I + (w'_e-\psi_e).\sum_{I=1}^{n=3}N_I(X_1).\delta\psi_I) + \\ & Q_e.(-\psi_e.\sum_{I=1}^{n=3}N'_I(X_1).\delta u_I + \sum_{I=1}^{n=3}N'_I(X_1).\delta w_I - (1+u'_e).\sum_{I=1}^{n=3}N_I(X_1).\delta\psi_I) + \\ & M_e.(\sum_{I=1}^{n=3}N'_I(X_1).\delta\psi_e)\Big]dX_1 - \int_0^{L_e}\Big[n_e.(\sum_{I=1}^{n=3}N_I(X_1).\delta u_I) + q_e.(\sum_{I=1}^{n=3}N_I(X_1).\delta w_I)\Big]dX_1\Big] = 0 \end{aligned}$$

$$\begin{aligned} \triangleright G(u,\eta) \approx \bigcup_{j=1}^{n_e}\Big[\frac{L_e}{2}.\sum_{I=1}^{n=3}\Big[\delta u_I \quad \delta w_I \quad \delta\psi_I\Big]\cdot\Big[\sum_{p=1}^{n_p}W_p.\begin{bmatrix} N'_I(\xi_p) & -N'_I(\xi_p)\psi_e & 0 \\ N'_I(\xi_p)\psi_e & N'_I(\xi_p) & 0 \\ (w'_e-\psi_e)N_I(\xi_p) & -(1+u'_e)N_I(\xi_p) & N'_I(\xi_p) \end{bmatrix}. \\ \begin{bmatrix} N_e \\ Q_e \\ M_e \end{bmatrix} - \sum_{p=1}^{n_p}W_p.\begin{bmatrix} N_I(\xi_p) & 0 & 0 \\ 0 & N_I(\xi_p) & 0 \\ 0 & 0 & N_I(\xi_p) \end{bmatrix}\cdot\begin{bmatrix} n_e \\ q_e \\ 0 \end{bmatrix}\Big]\Big] \approx 0 \end{aligned}$$

$$\triangleright G(u,\eta) \approx \bigcup_{j=1}^{n_e} \left[ \frac{L_e}{2} . \sum_{I=1}^{n=3} \boldsymbol{\eta}_I^T . \Big[ \sum_{p=1}^{n_p} W_p . \boldsymbol{B}_I^{S^T}(\xi_p, \boldsymbol{u}_I) . \boldsymbol{S}_e(\xi_p, \boldsymbol{u}_I) - \sum_{p=1}^{n_p} W_p . \boldsymbol{N}_I(\xi_p) . \boldsymbol{q}_e \Big] \right] \approx 0 \tag{3.14}$$

$$\boxed{G(u,\eta) \approx \bigcup_{j=1}^{n_e} \left[ \frac{L_e}{2} . \sum_{I=1}^{n=3} \boldsymbol{\eta}_I^T . \sum_{p=1}^{n_p} W_p . \Big[ \boldsymbol{B}_I^{S^T}(\xi_p, \boldsymbol{u}_I) . \boldsymbol{S}_e(\xi_p, \boldsymbol{u}_I) - \boldsymbol{N}_I(\xi_p) . \boldsymbol{q}_e \Big] \right] \approx 0} \tag{3.15}$$

## 3.5 Discretization of the Linearization of the Weak Form

Like previous chapter the tangential stiffness matrix is derived for the approximate theories. This leads for the formulation based on (3.7) with matrix $B_I^{S^T}$ from (3.13) to

$$\boxed{\begin{aligned} &DG(\boldsymbol{u},\boldsymbol{\eta}).\Delta \boldsymbol{u} \approx \bigcup_{j=1}^{n_e} \left[ \frac{L_e}{2} . \sum_{I=1}^{n=3} \sum_{K=1}^{n=3} \boldsymbol{\eta}_I^T . \Big[ \sum_{p=1}^{n_p} W_p . [\boldsymbol{B}_I^{S^T}(\xi_p) . \boldsymbol{D} . \boldsymbol{B}_K^S(\xi_p) + \\ &N_e(\xi_p) . \boldsymbol{G}_{IK}^{SN}(\xi_p) + Q_e(\xi_p) . \boldsymbol{G}_{IK}^{SQ}(\xi_p)] \Big] . \Delta \boldsymbol{u}_K \right] \end{aligned}} \tag{3.16}$$

and the compact format of tangent stiffness matrix is

$$\boxed{\begin{aligned} &K_{IK}^{tangent} \approx \bigcup_{j=1}^{n_e} \left[ \frac{L_e}{2} . \sum_{I=1}^{n=3} \sum_{K=1}^{n=3} \boldsymbol{\eta}_I^T . \Big[ \sum_{p=1}^{n_p} W_p . [\boldsymbol{B}_I^{S^T}(\xi_p) . \boldsymbol{D} . \boldsymbol{B}_K^S(\xi_p) + \\ &N_e(\xi_p) . \boldsymbol{G}_{IK}^{SN}(\xi_p) + Q_e(\xi_p) . \boldsymbol{G}_{IK}^{SQ}(\xi_p)] \Big] \right] \end{aligned}} \tag{3.17}$$

with

$$\begin{aligned} G_{IK}^{SN} &= \begin{bmatrix} 0 & 0 & 0 \\ 0 & 0 & N_I'(X_1).N_K(X_1) \\ 0 & N_I(X_1).N_K'(X_1) & -N_I(X_1).N_K(X_1) \end{bmatrix}, \\ G_{IK}^{SQ} &= \begin{bmatrix} 0 & 0 & -N_I'(X_1).N_K(X_1) \\ 0 & 0 & 0 \\ -N_I(X_1).N_K'(X_1) & 0 & 0 \end{bmatrix} \end{aligned} \tag{3.18}$$

This result can also be derived directly from equations (2.44) and (2.47) of the geometrically exact theory. In that case, the limits $\sin\psi \to \psi$ and $\cos\psi \to 1$ have to be computed for $\psi \to 0$.

# Chapter 4

# Euler-Bernoulli Beams

## 4.1 Kinematics

For the sake of completeness, the governing equations of the nonlinear bending of beam are developed from consideration. The classical beam theory is based on the Euler-Bernoulli hypothesis that plane sections perpendicular to the axis of the beam before deformation remain (a) plane, (b) rigid (not deform), and (c) rotate such that they remain perpendicular to the (deformed) axis after deformation. The assumptions amount to neglecting the Poisson effect and transverse strains. It means that $w' = \psi$. Therefore by applying this new restriction to equation (3.1) and also neglecting the strain part $u'$ in axial direction for shear strains the kinematic equation of Euler-Bernoulli Beam can be written:

$$\begin{aligned} &\epsilon(X_1) = u'(X_1) + \frac{1}{2}\psi^2(X_1), \\ &\gamma(X_1) = 0, \\ &\kappa(X_1) = \psi'(X_1) = w''(X_1) \end{aligned} \tag{4.1}$$

For simplicity $(X_1)$ will not be written in the rest of this chapter.

## 4.2 Weak Form of Equilibrium

The weak form of equilibrium which is equivalent to the principle of virtual work can be stated for shear elastic beams as

$$\begin{aligned} &G(u,\eta) = \int_0^l (N.\delta\epsilon + Q.\delta\gamma + M.\delta\kappa)dx - \int_0^l (n.\delta u + q.\delta w)dx = 0 \\ &\boldsymbol{S} = \begin{bmatrix} N \\ Q \\ M \end{bmatrix}, \delta\boldsymbol{\epsilon} = \begin{bmatrix} \delta\epsilon \\ \delta\gamma \\ \delta\kappa \end{bmatrix}, \boldsymbol{\eta} = \begin{bmatrix} \delta u \\ \delta w \\ \delta\psi \end{bmatrix}, \boldsymbol{q} = \begin{bmatrix} n \\ q \\ 0 \end{bmatrix} \end{aligned} \tag{4.2}$$

The virtual strains in (4.1) yields

$$\begin{aligned}\delta\epsilon &= \delta u' + w'\delta w' \\ \delta\gamma &= 0 \\ \delta\kappa &= \delta w''\end{aligned} \tag{4.3}$$

which leads, neglecting the shear term in (4.2) Thus the weak form related to Bernoulli beam is

$$G(u, w, \delta u, \delta w) = \int_0^l (N.(\delta u' + w'\delta w') + M.\delta w'')dx - \int_0^l (n.\delta u + q.\delta w)dx = 0 \tag{4.4}$$

and the stresses are defined as

$$N = EA.\epsilon = EA.(u' + \frac{1}{2}w'^2), \quad M = EI.\kappa = EI.w'' \tag{4.5}$$

therefore the first term of (4.4) can be specified as

$$\int_0^l \Big[[EA.(u' + \frac{1}{2}w'^2).\delta u'] + [EA.(u' + \frac{1}{2}w'^2).w'.\delta w'] + [EI.w''.\delta w'']\Big]dX_1 \tag{4.6}$$

and for future purposes the above weak form can also be written

$$\int_0^l \Big[EA.u'.\delta u' + \frac{1}{2}EA.w'.\delta u'.w' + EA.w'.\delta w'.u' + EI.w''.\delta w'' + \frac{1}{2}EA.w'.\delta w'.w'^2\Big]dX_1 \tag{4.7}$$

This differential relation is governing nonlinear bending of Bernoulli beam. Since analytic solutions are only available just for special cases, the finite element method will be implemented.

## 4.3 Finite Element Formulation

The strains (4.1) based on Bernoulli kinematics need shape for the deflection which are $C^1$-continuous since second order derivatives of the deflection $w$ with respect to the coordinate $X_1$ occurs in the strain measure. For simplicity $w$ and $\psi$ for an element with two nodes can be assigned with $\Omega$. See Figure (4.1)

$\Omega_1 = w_1 \quad \Omega_2 = \psi_1 \quad \Omega_3 = w_2 \quad \Omega_4 = \psi_2$

For the axial displacement $u$, a linear interpolation function $N_i$ is selected due to (2.9). For the deflection $\Omega$ cubical Hermite functions $H_I$ are applied, which are also used to discretize beam elements for the linear theory. Based on these functions, the following shape functions can be introduced for the deflection

▷ Cubical Hermite functions and corresponded derivations:

$$\begin{aligned}
&H_1(\xi_1) = \frac{1}{4}(2 - 3\xi_1 + \xi_1^3), \quad H_1'(\xi_1) = \frac{3}{4}(-1 + \xi^2), \quad H_1''(\xi_1) = \frac{3}{2}\xi \\
&H_2(\xi_1) = \frac{1}{4}(1 - \xi_1 - \xi^2 + \xi_1^3), \quad H_1'(\xi_1) = \frac{1}{4}(-1 - 2\xi_1 + 3\xi_1^2), \quad H_1''(\xi_1) = \frac{1}{2}(-1 + 3\xi_1)\xi_1 \\
&H_3(\xi_1) = \frac{1}{4}(2 + 3\xi_1 - \xi_1^3), \quad H_1'(\xi_1) = \frac{3}{4}(1 - \xi_1^2), \quad H_1''(\xi_1) = -\frac{3}{2}\xi_1 \\
&H_4(\xi_1) = \frac{1}{4}(-1 - \xi_1 + \xi_1^2 + \xi_1^3), \quad H_1'(\xi_1) = \frac{1}{4}(-1 + 2\xi_1 + 3\xi_1^2), \quad H_1''(\xi_1) = \frac{1}{2}(1 + 3\xi_1)\xi_1
\end{aligned} \tag{4.8}$$

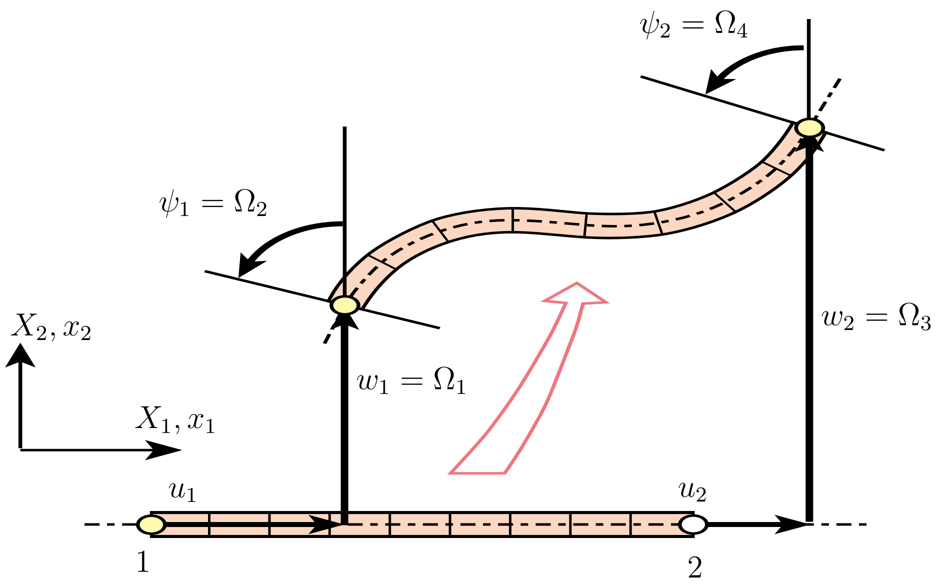


Figure 4.1: Two nodes Bernoulli Beam Element.

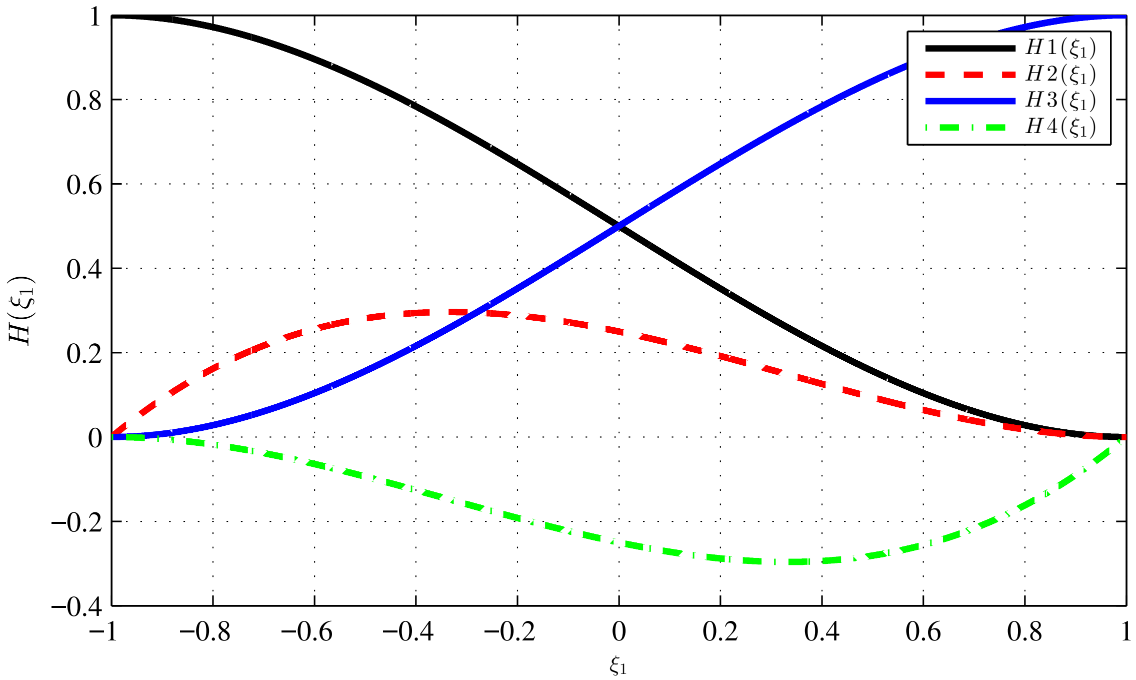


Figure 4.2: Cubic Hermite functions

The above functions are the Cubic Hermite function in $\xi_1$ coordination, but it has to be considered that for using the derivatives, the amount of first derivative and second derivative have to premultiply with $\frac{2}{L_e}$ and $\frac{4}{L_e^2}$ respectively. $L_e$ is the length of corresponded element. In fact these factors are necessary for transformation from physical coordination to natural coordination. It means

$$
\begin{aligned}
H_1'(\xi_1) &= \frac{3}{2L_e}(-1+\xi^2), \quad H_1''(\xi_1) = \frac{6}{L_e^2}\xi \\
H_1'(\xi_1) &= \frac{1}{2L_e}(-1-2\xi_1+3\xi_1^2), \quad H_1''(\xi_1) = \frac{2}{L_e^2}(-1+3\xi_1)\xi_1 \\
H_1'(\xi_1) &= \frac{3}{2L_e}(1-\xi_1^2), \quad H_1''(\xi_1) = -\frac{6}{L_e^2}\xi_1 \\
H_1'(\xi_1) &= \frac{1}{2L_e}(-1+2\xi_1+3\xi_1^2), \quad H_1''(\xi_1) = \frac{2}{L_e^2}(1+3\xi_1)\xi_1
\end{aligned}
\tag{4.9}
$$

Let the axial displacement of element $u_e$ and transverse deflection of element $w_e$ are interpolated as

$$
\begin{aligned}
u_e(\xi_1) &= \sum_{i=1}^{n=2} N_i(\xi_1).u_i = N_1(\xi_1).u_1 + N_2(\xi_1).u_2 \\
w_e(\xi_1) &= \sum_{I=1}^{m=4} H_I(\xi_1).\Omega_I = H_1(\xi_1).\Omega_1 + H_2(\xi_1).\Omega_2 + H_3(\xi_1).\Omega_3 + H_4(\xi_1).\Omega_4
\end{aligned}
\tag{4.10}
$$

moreover following interpolations also will be needed to derive the finite format

$$
\begin{aligned}
u_e'(\xi_1) &= \sum_{i=1}^{n=2} N_i'(\xi_1).u_i = N_1'(\xi_1).u_1 + N_2'(\xi_1).u_2 \\
\delta u_e'(\xi_1) &= \sum_{i=1}^{n=2} N_i'(\xi_1).\delta u_i = N_1'(\xi_1).\delta u_1 + N_2'(\xi_1).\delta u_2 \\
w_e'(\xi_1) &= \sum_{I=1}^{m=4} H_I'(\xi_1).\Omega_I = H_1'(\xi_1).\Omega_1 + H_2'(\xi_1).\frac{L_e}{2}\Omega_2 + H_3'(\xi_1).\Omega_3 + H_4'(\xi_1).\frac{L_e}{2}\Omega_4 \\
w_e''(\xi_1) &= \sum_{I=1}^{m=4} H_I''(\xi_1).\Omega_I = H_1''(\xi_1).\Omega_1 + H_2''(\xi_1).\frac{L_e}{2}\Omega_2 + H_3''(\xi_1).\Omega_3 + H_4''(\xi_1).\frac{L_e}{2}\Omega_4 \\
\delta w_e'(\xi_1) &= \sum_{I=1}^{m=4} H_I'(\xi_1).\delta\Omega_I = H_1'(\xi_1).\delta\Omega_1 + H_2'(\xi_1).\frac{L_e}{2}\delta\Omega_2 + H_3'(\xi_1).\delta\Omega_3 + H_4'(\xi_1).\frac{L_e}{2}\delta\Omega_4 \\
\delta w_e''(\xi_1) &= \sum_{I=1}^{m=4} H_I''(\xi_1).\delta\Omega_I = H_1''(\xi_1).\delta\Omega_1 + H_2''(\xi_1).\frac{L_e}{2}\delta\Omega_2 + H_3''(\xi_1).\delta\Omega_3 + H_4''(\xi_1).\frac{L_e}{2}\delta\Omega_4
\end{aligned}
\tag{4.11}
$$

## 4.4 Weak Form in terms of Nodal Quantities $\boldsymbol{u}_I$ and $\Omega_I$

The weak form for an element in $\xi_1$ coordination based on relation (4.7) can be written

$$\int_0^{L_e}\Big[EA.u'_e.\delta u'_e+\frac{1}{2}EA.w'_e.\delta u'_e.w'_e+EA.w'_e.\delta w'_e.u'_e+EI.w''_e.\delta w''_e+\frac{1}{2}EA.w'_e.\delta w'_e.w'^2_e\Big].\frac{L_e}{2}d\xi_1 \tag{4.12}$$

By inserting the equation (4.11) in weak form (4.12), the following relation will be resulted

$$\begin{aligned}
&\int_0^{L_e}\Big[EA.(\sum_{i=1}^{n=2}\sum_{j=1}^{n=2}N'_i.N'_j.u_j.\delta u_i)\Big]\frac{L_e}{2}d\xi_1+\\
\frac{1}{2}&\int_0^{L_e}\Big[EA.w'_e.(\sum_{i=1}^{n=2}\sum_{J=1}^{m=4}N'_i.H'_J.\delta u_i.\Omega_J)\Big]\frac{L_e}{2}d\xi_1+\\
&\int_0^{L_e}\Big[EA.w'_e.(\sum_{I=1}^{m=4}\sum_{j=1}^{n=2}N'_j.H'_I.u_i.\delta\Omega_J)\Big]\frac{L_e}{2}d\xi_1+\\
&\int_0^{L_e}\Big[EI.(\sum_{I=1}^{m=4}\sum_{J=1}^{m=4}H''_I.H''_J.\Omega_I.\delta\Omega_J)\Big]\frac{L_e}{2}d\xi_1+\\
\frac{1}{2}&\int_0^{L_e}\Big[EA.w'^2_e.(\sum_{I=1}^{m=4}\sum_{J=1}^{m=4}H'_I.H'_J.\Omega_I.\delta\Omega_J)\Big]\frac{L_e}{2}d\xi_1
\end{aligned} \tag{4.13}$$

It can be realized that $i,j=1,2$ and $I,J=1,2,3,4$, therefore we write it in matrix form

$$\begin{bmatrix}\delta u_1 & \delta u_2\end{bmatrix}\underbrace{\int_0^{L_e}EA\begin{bmatrix}N'_1N'_1 & N'_1N'_2\\ N'_2N'_1 & N'_2N'_2\end{bmatrix}\frac{L_e}{2}d\xi_1}_{\boldsymbol{k}^{11}}\begin{bmatrix}u_1\\ u_2\end{bmatrix}+$$

$$\begin{bmatrix}\delta u_1 & \delta u_2\end{bmatrix}\underbrace{\int_0^{L_e}\frac{1}{2}EA.w'_e\begin{bmatrix}N'_1H'_1 & N'_1H'_2 & N'_1H'_3 & N'_1H'_4\\ N'_2H'_1 & N'_2H'_2 & N'_2H'_3 & N'_2H'_4\end{bmatrix}\frac{L_e}{2}d\xi_1}_{\boldsymbol{k}^{12}}\begin{bmatrix}\Omega_1\\ \Omega_2\\ \Omega_3\\ \Omega_4\end{bmatrix}+$$

$$\begin{bmatrix}\delta\Omega_1 & \delta\Omega_2 & \delta\Omega_3 & \delta\Omega_4\end{bmatrix}\underbrace{\int_0^{L_e}EA.w'_e\begin{bmatrix}N'_1H'_1 & N'_2H'_1\\ N'_1H'_2 & N'_2H'_2\\ N'_1H'_3 & N'_2H'_3\\ N'_1H'_4 & N'_2H'_4\end{bmatrix}\frac{L_e}{2}d\xi_1}_{\boldsymbol{k}^{21}}\begin{bmatrix}u_1\\ u_2\end{bmatrix}+$$

(continued on next page)

(continued from previous page)

$$\begin{bmatrix}\delta\Omega_1 & \delta\Omega_2 & \delta\Omega_3 & \delta\Omega_4\end{bmatrix} \underbrace{\int_0^{L_e} EI \begin{bmatrix} H_1''H_1'' & H_1''H_2'' & H_1''H_3'' & H_1''H_4'' \\ H_2''H_1'' & H_2''H_2'' & H_2''H_3'' & H_2''H_4'' \\ H_3''H_1'' & H_3''H_2'' & H_3''H_3'' & H_3''H_4'' \\ H_4''H_1'' & H_4''H_2'' & H_4''H_3'' & H_4''H_4'' \end{bmatrix} \frac{L_e}{2} d\xi_1}_{\boldsymbol{k}^{22^{(1)}}} \begin{bmatrix}\Omega_1 \\ \Omega_2 \\ \Omega_3 \\ \Omega_4\end{bmatrix} +$$

$$\begin{bmatrix}\delta\Omega_1 & \delta\Omega_2 & \delta\Omega_3 & \delta\Omega_4\end{bmatrix} \underbrace{\int_0^{L_e} \frac{1}{2} EA.w_e'^2 \begin{bmatrix} H_1'H_1' & H_1'H_2' & H_1'H_3' & H_1'H_4' \\ H_2'H_1' & H_2'H_2' & H_2'H_3' & H_2'H_4' \\ H_3'H_1' & H_3'H_2' & H_3'H_3' & H_3'H_4' \\ H_4'H_1' & H_4'H_2' & H_4'H_3' & H_4'H_4' \end{bmatrix} \frac{L_e}{2} d\xi_1}_{\boldsymbol{k}^{22^{(2)}}} \begin{bmatrix}\Omega_1 \\ \Omega_2 \\ \Omega_3 \\ \Omega_4\end{bmatrix} \tag{4.14}$$

The stiffness matrix of one element for beam based on Bernoulli theory $\boldsymbol{k}^B$ can be expressed

$$\begin{bmatrix}\delta\boldsymbol{u}_i & \delta\boldsymbol{\Omega}_I\end{bmatrix} \underbrace{\left[\begin{array}{c|c} \boldsymbol{k}^{11} & \boldsymbol{k}^{12} \\ \hline \boldsymbol{k}^{21} & \boldsymbol{k}^{22^{(1)}} + \boldsymbol{k}^{22^{(2)}} \end{array}\right]}_{\boldsymbol{k}^B} \underbrace{\begin{bmatrix}\boldsymbol{u}_i \\ \boldsymbol{\Omega}_I\end{bmatrix}}_{\boldsymbol{\Lambda}} = \begin{bmatrix}\delta\boldsymbol{u}_i & \delta\boldsymbol{\Omega}_I\end{bmatrix} \begin{bmatrix}\boldsymbol{F}^1 \\ \boldsymbol{F}^2\end{bmatrix} \quad \text{with}$$

$$k_B = \left[\begin{array}{c|c|c|c|c|c} k_{11}^{11} & k_{12}^{11} & k_{11}^{12} & k_{12}^{12} & k_{13}^{12} & k_{14}^{12} \\ \hdashline k_{21}^{11} & k_{22}^{11} & k_{21}^{12} & k_{22}^{12} & k_{23}^{12} & k_{24}^{12} \\ \hdashline k_{11}^{21} & k_{12}^{21} & k_{11}^{22^{(1)}} + k_{11}^{22^{(2)}} & k_{12}^{22^{(1)}} + k_{12}^{22^{(2)}} & k_{13}^{22^{(1)}} + k_{13}^{22^{(2)}} & k_{14}^{22^{(1)}} + k_{14}^{22^{(2)}} \\ \hdashline k_{21}^{21} & k_{22}^{21} & k_{21}^{22^{(1)}} + k_{21}^{22^{(2)}} & k_{22}^{22^{(1)}} + k_{22}^{22^{(2)}} & k_{23}^{22^{(1)}} + k_{23}^{22^{(2)}} & k_{24}^{22^{(1)}} + k_{24}^{22^{(2)}} \\ \hdashline k_{31}^{21} & k_{32}^{21} & k_{31}^{22^{(1)}} + k_{31}^{22^{(2)}} & k_{32}^{22^{(1)}} + k_{32}^{22^{(2)}} & k_{33}^{22^{(1)}} + k_{33}^{22^{(2)}} & k_{34}^{22^{(1)}} + k_{34}^{22^{(2)}} \\ \hdashline k_{41}^{21} & k_{42}^{21} & k_{41}^{22^{(1)}} + k_{41}^{22^{(2)}} & k_{42}^{22^{(1)}} + k_{42}^{22^{(2)}} & k_{43}^{22^{(1)}} + k_{43}^{22^{(2)}} & k_{44}^{22^{(1)}} + k_{44}^{22^{(2)}} \end{array}\right], \quad \begin{bmatrix}\boldsymbol{u}_i \\ \boldsymbol{\Omega}_I\end{bmatrix} = \begin{bmatrix} u_1 \\ u_2 \\ \Omega_1 \\ \Omega_2 \\ \Omega_3 \\ \Omega_4 \end{bmatrix} \tag{4.15}$$

We also note that $(\boldsymbol{k}^{12})^T \neq \boldsymbol{k}^{21}$. The coefficient matrices $\boldsymbol{k}^{12}$, $\boldsymbol{k}^{21}$, and $\boldsymbol{k}^{22^{(2)}}$ are functions of the unknown displacement $w$. When the non linearity is not considered, we will have $\boldsymbol{k}^{12} = 0$ and $\boldsymbol{k}^{21} = 0$, and the equation (4.15)[1] involving $\boldsymbol{u}_i$ (the bar problem) are uncoupled from those involving $\boldsymbol{\Omega}_I$ (the beam problem), and therefore, they can be solved independent of each other:

$$\boldsymbol{k}^{11}.\boldsymbol{u}_i = \boldsymbol{F}^1, \qquad \boldsymbol{k}^{22^{(1)}}.\boldsymbol{\Omega}_I = \boldsymbol{F}^2 \tag{4.16}$$

When non linearity is accounted for, the equations are coupled (for example bending and stretching deformations of the beam are coupled) and non linear. Therefore, an iterative method must be used to solve the assembled equations. When these matrix coefficients are evaluated using equation $(4.10)^2$ from the previous iteration, we say that the equations are linearized.
For future programming purposes it is better to rearrange the matrix and vector, we obtain

$$\left[\begin{array}{c|c|c|c|c|c}
k_{11}^{11} & k_{11}^{12} & k_{12}^{12} & k_{12}^{11} & k_{13}^{12} & k_{14}^{12} \\
\hline
k_{11}^{21} & k_{11}^{22(1)} + k_{11}^{22(2)} & k_{12}^{22(1)} + k_{12}^{22(2)} & k_{12}^{21} & k_{13}^{22(1)} + k_{13}^{22(2)} & k_{14}^{22(1)} + k_{14}^{22(2)} \\
\hline
k_{21}^{21} & k_{21}^{22(1)} + k_{21}^{22(2)} & k_{22}^{22(1)} + k_{22}^{22(2)} & k_{22}^{21} & k_{23}^{22(1)} + k_{23}^{22(2)} & k_{24}^{22(1)} + k_{24}^{22(2)} \\
\hline
k_{21}^{11} & k_{21}^{12} & k_{22}^{12} & k_{22}^{11} & k_{23}^{12} & k_{24}^{12} \\
\hline
k_{31}^{21} & k_{31}^{22(1)} + k_{31}^{22(2)} & k_{32}^{22(1)} + k_{32}^{22(2)} & k_{32}^{21} & k_{33}^{22(1)} + k_{33}^{22(2)} & k_{34}^{22(1)} + k_{34}^{22(2)} \\
\hline
k_{41}^{21} & k_{41}^{22(1)} + k_{41}^{22(2)} & k_{42}^{22(1)} + k_{42}^{22(2)} & k_{42}^{21} & k_{43}^{22(1)} + k_{43}^{22(2)} & k_{44}^{22(1)} + k_{44}^{22(2)}
\end{array}\right] . \begin{bmatrix} u_1 \\ \Omega_1 \\ \Omega_2 \\ u_2 \\ \Omega_3 \\ \Omega_4 \end{bmatrix} \tag{4.17}$$

## 4.5 Discretization of the Linearization of the Weak Form

The complete linearization of weak form (4.4) can be derived with constitutive equation in equation (4.5). we obtain

$$DG(u, w, \delta u, \delta w).\Delta\mathbf{\Lambda} = \int_0^l (\delta\epsilon.EA.\Delta\epsilon + \delta\kappa.EI.\Delta\kappa)dX_1 + \int_0^l (\Delta\delta\epsilon.N + \Delta\delta\kappa.M)dX_1 \tag{4.18}$$

The parameters $\delta\epsilon$, $\delta\kappa$, $N$ and $M$ are described in equations $(4.3)^1$, $(4.3)^3$, $(4.5)^1$ and $(4.5)^2$ respectively. But the following parameters will be needed.

$$\begin{aligned} \Delta\epsilon &= \Delta u' + w'.\Delta w' \\ \Delta\kappa &= \Delta w'' \end{aligned} \tag{4.19}$$

and

$$\begin{aligned} \Delta\delta\epsilon &= \delta w'.\Delta w' \\ \Delta\delta\kappa &= 0 \end{aligned} \tag{4.20}$$

and for an element it can be clearly written

$$\begin{aligned} \Delta\epsilon_e &= \Delta u_e' + w_e'.\Delta w_e' \\ \Delta\kappa_e &= \Delta w_e'' \end{aligned} \tag{4.21}$$

and

$$\begin{aligned} \Delta\delta\epsilon_e &= \delta w_e'.\Delta w_e' \\ \Delta\delta\kappa_e &= 0 \end{aligned} \tag{4.22}$$

The following interpolations also will be needed to derive the finite format

$$
\begin{aligned}
\Delta u'_e(\xi_1) &= \sum_{i=1}^{n=2} N'_i(\xi_1).\Delta u_i = N'_1(\xi_1).\Delta u_1 + N'_2(\xi_1).\Delta u_2 \\
\Delta w'_e(\xi_1) &= \sum_{I=1}^{m=4} H'_I(\xi_1).\Delta\Omega_I = H'_1(\xi_1).\Delta\Omega_1 + H'_2(\xi_1).\frac{L_e}{2}\Delta\Omega_2 + H'_3(\xi_1).\Delta\Omega_3 + H'_4(\xi_1).\frac{L_e}{2}\Delta\Omega_4 \\
\Delta w''_e(\xi_1) &= \sum_{I=1}^{m=4} H''_I(\xi_1).\Delta\Omega_I = H''_1(\xi_1).\Delta\Omega_1 + H''_2(\xi_1).\frac{L_e}{2}\Delta\Omega_2 + H''_3(\xi_1).\Delta\Omega_3 + H''_4(\xi_1).\frac{L_e}{2}\Delta\Omega_4
\end{aligned}
\tag{4.23}
$$

By inserting the above equations in equation (4.17) we obtain

$$
\begin{aligned}
DG(u,w,\delta u,\delta w).\Delta\boldsymbol{\Lambda} = &\int_0^l (\delta u' + w'.\delta w').EA.(\Delta u' + w'.\Delta w')dX_1 + \\
&\int_0^l \delta w''.EI.\Delta w'' dX_1 + \int_0^l \delta w'.\Delta w'.N dX_1
\end{aligned}
\tag{4.24}
$$

For derivation of tangent stiffness matrix, equation (4.23) for one element can be expanded

$$
\begin{aligned}
&\int_0^{L_e} [EA.\delta u'_e.\Delta u'_e + EA.w'_e.\delta u'_e.\Delta w'_e + EA.w'_e.\Delta u'_e.\delta w'_e + EI.\delta w''_e.\Delta w''_e + \\
&\quad \frac{1}{2}EA.w'^2_e.\Delta w'_e.\delta w'_e + EA.w'^2_e.\delta w'_e.\Delta w'_e + EA.u'_e.\Delta w'_e.\delta w'_e]dX_1
\end{aligned}
\tag{4.25}
$$

By inserting equations (4.11) and (4.22) to above formulation we obtain

$$
\begin{aligned}
&\int_0^{L_e} \Big[EA.(\sum_{i=1}^{n=2}\sum_{j=1}^{n=2} N'_i.N'_j.\delta u_j.\Delta u_i)\Big]\frac{L_e}{2}d\xi_1 + \\
&\int_0^{L_e} \Big[EA.w'_e.(\sum_{i=1}^{n=2}\sum_{J=1}^{m=4} N'_i.H'_J.\delta u_i.\Delta\Omega_J)\Big]\frac{L_e}{2}d\xi_1 + \\
&\int_0^{L_e} \Big[EA.w'_e.(\sum_{I=1}^{m=4}\sum_{j=1}^{n=2} N'_j.H'_I.\Delta u_i.\delta\Omega_J)\Big]\frac{L_e}{2}d\xi_1 + \\
&\int_0^{L_e} \Big[EI.(\sum_{I=1}^{m=4}\sum_{J=1}^{m=4} H''_I.H''_J.\Delta\Omega_I.\delta\Omega_J)\Big]\frac{L_e}{2}d\xi_1 + \\
\frac{1}{2}&\int_0^{L_e} \Big[EA.w'^2_e.(\sum_{I=1}^{m=4}\sum_{J=1}^{m=4} H'_I.H'_J.\Delta\Omega_I.\delta\Omega_J)\Big]\frac{L_e}{2}d\xi_1 + \\
&\int_0^{L_e} \Big[EA.w'^2_e.(\sum_{I=1}^{m=4}\sum_{J=1}^{m=4} H'_I.H'_J.\delta\Omega_I.\Delta\Omega_J)\Big]\frac{L_e}{2}d\xi_1 + \\
&\int_0^{L_e} \Big[EA.u'_e.(\sum_{I=1}^{m=4}\sum_{J=1}^{m=4} H'_I.H'_J.\Delta\Omega_I.\delta\Omega_J)\Big]\frac{L_e}{2}d\xi_1
\end{aligned}
\tag{4.26}
$$

It can be realized that $i, j = (1, 2)$ and $I, J = (1, 2, 3, 4)$, therefore it can also be written in matrix

$$
\begin{bmatrix} \delta u_1 & \delta u_2 \end{bmatrix} \underbrace{\int_0^{L_e} EA \begin{bmatrix} N_1' N_1' & N_1' N_2' \\ N_2' N_1' & N_2' N_2' \end{bmatrix} \frac{L_e}{2} d\xi_1}_{\boldsymbol{t}^{11} = \boldsymbol{k}^{11}} \begin{bmatrix} \Delta u_1 \\ \Delta u_2 \end{bmatrix} +
$$

$$
\begin{bmatrix} \delta u_1 & \delta u_2 \end{bmatrix} \underbrace{\int_0^{L_e} EA.w_e' \begin{bmatrix} N_1' H_1' & N_1' H_2' & N_1' H_3' & N_1' H_4' \\ N_2' H_1' & N_2' H_2' & N_2' H_3' & N_2' H_4' \end{bmatrix} \frac{L_e}{2} d\xi_1}_{\boldsymbol{t}^{12} = 2.\boldsymbol{k}^{12}} \begin{bmatrix} \Delta\Omega_1 \\ \Delta\Omega_2 \\ \Delta\Omega_3 \\ \Delta\Omega_4 \end{bmatrix} +
$$

$$
\begin{bmatrix} \delta\Omega_1 & \delta\Omega_2 & \delta\Omega_3 & \delta\Omega_4 \end{bmatrix} \underbrace{\int_0^{L_e} EA.w_e' \begin{bmatrix} N_1' H_1' & N_2' H_1' \\ N_1' H_2' & N_2' H_2' \\ N_1' H_3' & N_2' H_3' \\ N_1' H_4' & N_2' H_4' \end{bmatrix} \frac{L_e}{2} d\xi_1}_{\boldsymbol{t}^{21} = \boldsymbol{k}^{21}} \begin{bmatrix} \Delta u_1 \\ \Delta u_2 \end{bmatrix} +
$$

$$
\begin{bmatrix} \delta\Omega_1 & \delta\Omega_2 & \delta\Omega_3 & \delta\Omega_4 \end{bmatrix} \underbrace{\int_0^{L_e} EI \begin{bmatrix} H_1'' H_1'' & H_1'' H_2'' & H_1'' H_3'' & H_1'' H_4'' \\ H_2'' H_1'' & H_2'' H_2'' & H_2'' H_3'' & H_2'' H_4'' \\ H_3'' H_1'' & H_3'' H_2'' & H_3'' H_3'' & H_3'' H_4'' \\ H_4'' H_1'' & H_4'' H_2'' & H_4'' H_3'' & H_4'' H_4'' \end{bmatrix} \frac{L_e}{2} d\xi_1}_{\boldsymbol{t}^{22^{(1)}} = \boldsymbol{k}^{22^{(1)}}} \begin{bmatrix} \Delta\Omega_1 \\ \Delta\Omega_2 \\ \Delta\Omega_3 \\ \Delta\Omega_4 \end{bmatrix} +
$$

$$
\begin{bmatrix} \delta\Omega_1 & \delta\Omega_2 & \delta\Omega_3 & \delta\Omega_4 \end{bmatrix} \underbrace{\int_0^{L_e} \frac{1}{2} EA.w_e'^2 \begin{bmatrix} H_1' H_1' & H_1' H_2' & H_1' H_3' & H_1' H_4' \\ H_2' H_1' & H_2' H_2' & H_2' H_3' & H_2' H_4' \\ H_3' H_1' & H_3' H_2' & H_3' H_3' & H_3' H_4' \\ H_4' H_1' & H_4' H_2' & H_4' H_3' & H_4' H_4' \end{bmatrix} \frac{L_e}{2} d\xi_1}_{\boldsymbol{t}^{22^{(2)^1}} = \boldsymbol{k}^{22^{(2)}}} \begin{bmatrix} \Delta\Omega_1 \\ \Delta\Omega_2 \\ \Delta\Omega_3 \\ \Delta\Omega_4 \end{bmatrix} +
$$

(continued on next page)

(continued from previous page)

$$
\begin{bmatrix}\delta\Omega_1 & \delta\Omega_2 & \delta\Omega_3 & \delta\Omega_4\end{bmatrix}\underbrace{\int_0^{L_e} EA.w_e'^2 \begin{bmatrix} H_1'H_1' & H_1'H_2' & H_1'H_3' & H_1'H_4' \\ H_2'H_1' & H_2'H_2' & H_2'H_3' & H_2'H_4' \\ H_3'H_1' & H_3'H_2' & H_3'H_3' & H_3'H_4' \\ H_4'H_1' & H_4'H_2' & H_4'H_3' & H_4'H_4' \end{bmatrix} \frac{L_e}{2} d\xi_1}_{\boldsymbol{t}^{22^{(2)^2}} = 2.\boldsymbol{k}^{22^{(2)}}} \begin{bmatrix}\Delta\Omega_1 \\ \Delta\Omega_2 \\ \Delta\Omega_3 \\ \Delta\Omega_4\end{bmatrix} +
$$

$$
\begin{bmatrix}\delta\Omega_1 & \delta\Omega_2 & \delta\Omega_3 & \delta\Omega_4\end{bmatrix}\underbrace{\int_0^{L_e} EA.u_e' \begin{bmatrix} H_1'H_1' & H_1'H_2' & H_1'H_3' & H_1'H_4' \\ H_2'H_1' & H_2'H_2' & H_2'H_3' & H_2'H_4' \\ H_3'H_1' & H_3'H_2' & H_3'H_3' & H_3'H_4' \\ H_4'H_1' & H_4'H_2' & H_4'H_3' & H_4'H_4' \end{bmatrix} \frac{L_e}{2} d\xi_1}_{\boldsymbol{t}^{22^{(3)}}} \begin{bmatrix}\Delta\Omega_1 \\ \Delta\Omega_2 \\ \Delta\Omega_3 \\ \Delta\Omega_4\end{bmatrix}
\tag{4.27}
$$

The tangent stiffness matrix of one element for beam based on Bernoulli theory $\boldsymbol{t}^B$ can be expressed

$$
\begin{bmatrix}\delta\boldsymbol{u}_i & \delta\boldsymbol{\Omega}_I\end{bmatrix}\underbrace{\left[\begin{array}{c|c} \boldsymbol{t}^{11} & \boldsymbol{t}^{12} \\ \hline \boldsymbol{t}^{21} & \boldsymbol{t}^{22^{(1)}} + \underbrace{\boldsymbol{t}^{22^{(2)^1}} + \boldsymbol{t}^{22^{(2)^2}}}_{\boldsymbol{t}^{22^{(2)}}} + \boldsymbol{t}^{22^{(3)}} \end{array}\right]}_{\boldsymbol{t}^B}\underbrace{\begin{bmatrix}\Delta\boldsymbol{u}_i \\ \Delta\boldsymbol{\Omega}_I\end{bmatrix}}_{\Delta\boldsymbol{\Lambda}}
\tag{4.28}
$$

with

$$
\begin{bmatrix}\Delta\boldsymbol{u}_i & \Delta\boldsymbol{\Omega}_I\end{bmatrix}^T = \begin{bmatrix}\Delta u_1 & \Delta u_2 & \Delta\Omega_1 & \Delta\Omega_2 & \Delta\Omega_3 & \Delta\Omega_4\end{bmatrix}^T
$$

and

$$
\boldsymbol{t}^B = \left[\begin{array}{c|c|c|c|c|c}
t^{11}_{11} & t^{11}_{12} & t^{12}_{11} & t^{12}_{12} & t^{12}_{13} & t^{12}_{14} \\ \hdashline
t^{11}_{21} & t^{11}_{22} & t^{12}_{21} & t^{12}_{22} & t^{12}_{23} & t^{12}_{24} \\ \hdashline
t^{21}_{11} & t^{21}_{12} & t^{22^{(1)}}_{11} + t^{22^{(2)}}_{11} + t^{22^{(3)}}_{11} & t^{22^{(1)}}_{12} + t^{22^{(2)}}_{12} + t^{22^{(3)}}_{12} & t^{22^{(1)}}_{13} + t^{22^{(2)}}_{13} + t^{22^{(3)}}_{13} & t^{22^{(1)}}_{14} + t^{22^{(2)}}_{14} + t^{22^{(3)}}_{14} \\ \hdashline
t^{21}_{21} & t^{21}_{22} & t^{22^{(1)}}_{21} + t^{22^{(2)}}_{21} + t^{22^{(3)}}_{21} & t^{22^{(1)}}_{22} + t^{22^{(2)}}_{22} + t^{22^{(3)}}_{22} & t^{22^{(1)}}_{23} + t^{22^{(2)}}_{23} + t^{22^{(3)}}_{23} & t^{22^{(1)}}_{24} + t^{22^{(2)}}_{24} + t^{22^{(3)}}_{24} \\ \hdashline
t^{21}_{31} & t^{21}_{32} & t^{22^{(1)}}_{31} + t^{22^{(2)}}_{31} + t^{22^{(3)}} & t^{22^{(1)}}_{32} + t^{22^{(2)}}_{32} + t^{22^{(3)}}_{32} & t^{22^{(1)}}_{33} + t^{22^{(2)}}_{33} + t^{22^{(3)}}_{33} & t^{22^{(1)}}_{34} + t^{22^{(2)}}_{34} + t^{22^{(3)}}_{34} \\ \hdashline
t^{21}_{41} & t^{21}_{42} & t^{22^{(1)}}_{41} + t^{22^{(2)}}_{41} + t^{22^{(3)}}_{41} & t^{22^{(1)}}_{42} + t^{22^{(2)}}_{42} + t^{22^{(3)}}_{42} & t^{22^{(1)}}_{43} + t^{22^{(2)}}_{43} + t^{22^{(3)}}_{43} & t^{22^{(1)}}_{44} + t^{22^{(2)}}_{44} + t^{22^{(3)}}_{44}
\end{array}\right]
\tag{4.29}
$$

## 4.6 Memrane Locking

For the linear case, the axial displacement $u$ is uncoupled from the bending deflection $w$, and they can be determined independently from the finite element equations respectively. [See equations (4.16)]. Matrices $\boldsymbol{k}^{11}$ and $\boldsymbol{k}^{22^{(1)}}$ are the linear stiffness coefficients. Under the assumption of linearity, if a beam is subjected to only bending loads and no axial loads, then $u = 0$ [when $u$ is specified to be zero at least at one point]. In other words, in linear case a hinged-hinged beam and a pinned-pinned beam will have the same deflection $w$ under the same load and $u = 0$ for all points of beam. However, this is not true when the non linearity is included. In fact the coupling between $u$ and $w$ will cause the beam to undergo axial displacement even when there are no axial forces, and the solution $(u, w)$ will be different for the two cases shown in Figure (4.3)
First of all we know that the hinged-hinged beam does not have any end constrains on $u$ and

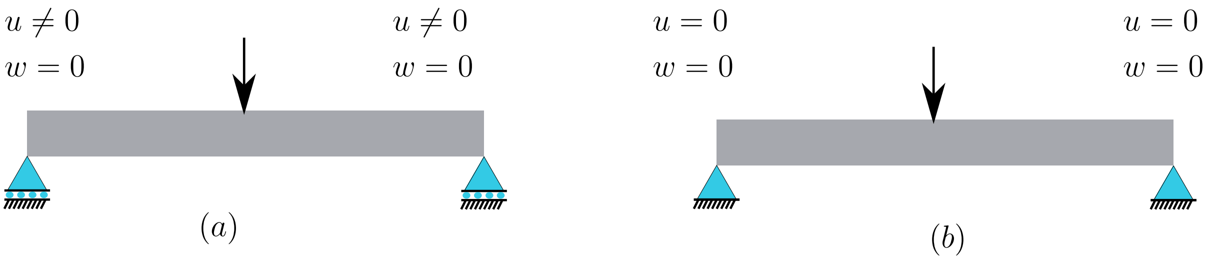


*Figure 4.3: (a) Hinged-Hinged Beam and (b) Pinned-Pinned Beam*

a transverse load does not induce any axial strain, therefore $\epsilon = 0$ because the beam is free to side on the rollers to accommodate transverse deflection. Second of all the pinned-pinned beam is restricted from axial movement at $X_1 = 0$ and $X_1 = L$. As a result, it will develop axial strain to accommodate the transverse deflection. Thus a hinged-hinged beam will have larger transverse deflection than a pinned-pinned beam.
Let us examine the requirement that for a hinged-hinged beam.

$$\epsilon = u' + \frac{1}{2}w'^2 = 0 \tag{4.30}$$

In order to satisfy the constraint in (4.30), we must have

$$-u' \approx w'^2 \tag{4.31}$$

Based on similarity, for integration (4.31) on length the same degree of polynomial for $u'$ and $w'^2$ have to be used. For example, when $w$ is interpolated using Hermite Cubic polynomial, then $w'^2$ is a fourth-order polynomial. Hence, $u'$ should be a fourth-order polynomial (or $u$ should be a fifth-order polynomial). Approximation of $u$ with any polynomial less than the fifth-order and $w$ with Hermite cubic polynomials, the constraint in equation (4.31) is clearly not satisfied and resulting element stiffness matrix will be stiff and the element said to be locked and this phenomenon is known as the membrane locking.
A practical way to satisfy the constraint in equation (4.31) is to use the minimum interpolation of $u$ and $w$ (it means linear interpolation of $u$ and Hermite cubic interpolation of $w$) but treat $\epsilon$ as a constant. This may seem impossible, but it is possible from a numerical point of view. Since $u'$ is constant, it is necessary to treat $w'^2$ as a constant in the numerical evaluation of element stiffness coefficient. Thus if $EA$ is a constant, all non-linear stiffness coefficients

should be evaluated using one-point Gauss quadrature. These coefficients include $\boldsymbol{k}^{12}$, $\boldsymbol{k}^{21}$, $\boldsymbol{k}^{22^{(2)}}$, $\boldsymbol{t}^{12}$, $\boldsymbol{t}^{21}$, $\boldsymbol{t}^{22^{(2)^1}}$, $\boldsymbol{t}^{22^{(2)^2}}$ and $\boldsymbol{t}^{22^{(3)}}$. Other terms like $\boldsymbol{k}^{11}$, $\boldsymbol{k}^{22^{(1)}}$, $\boldsymbol{t}^{11}$ and $\boldsymbol{t}^{22^{(1)}}$ may be evaluated exactly using two-point quadrature for for constant values $EA$ and $EI$.

# Chapter 5

# Second Order Beam Theory

## 5.1 Kinematics

The kinematic of Second Order Beam Theory is

$$
\begin{aligned}
&\epsilon(X_1) = u'(X_1) + \frac{1}{2}\psi^2(X_1), \\
&\gamma(X_1) = 0, \\
&\kappa(X_1) = \psi'(X_1) = w''(X_1)
\end{aligned}
\tag{5.1}
$$

For simplicity $(X_1)$ will not be written in the rest of this chapter.

## 5.2 Weak Form of Equilibrium

The virtual strains in (5.1) yields

$$
\begin{aligned}
&\delta\epsilon = \delta u' + w'\delta w' \\
&\delta\gamma = 0 \\
&\delta\kappa = \delta w''
\end{aligned}
\tag{5.2}
$$

and the weak form is expressed

$$G(u, w, \delta u, \delta w) = \int_0^l (N.(\delta u' + w'\delta w') + M.\delta w'')dx - \int_0^l (n.\delta u + q.\delta w)dx = 0 \tag{5.3}$$

and the stresses are defined as

$$N = EA.\epsilon = EA.(u' + \frac{1}{2}w'^2), \quad M = EI.\kappa = EI.w'' \tag{5.4}$$

But in this section the normal stress is split into a linear part $EA.u'$ and a non-linear part $N.w'.\delta w'$.

$$G(u, w, \delta u, \delta w) = \int_0^l (\delta u'.EA.u' + N.w'.\delta w' + \delta w''.EI.w'')dx - \int_0^l (n.\delta u + q.\delta w)dx = 0 \tag{5.5}$$

Here it is assumed that the normal stress is constant within each load step.

## 5.3 Weak Form in terms of Nodal Quantities $u_I$ and $\Omega_I$

The weak form for an element in $\xi_1$ coordination based on first term of relation (5.5) can be written

$$\int_0^{L_e} (\delta u'_e.EA.u'_e + N.w'_e.\delta w'_e + \delta w''_e.EI.w''_e)dX_1 \tag{5.6}$$

By inserting equations (4.11)$^1$ for $u'_e$, (4.11)$^2$ for $\delta u'_e$, (4.11)$^3$ for $w'_e$,(4.11)$^5$ for $\delta w'_e$, (4.11)$^4$ for $w''_e$ and (4.11)$^6$ for $\delta w''_e$ and also neglecting the non-linear part of $N$, more precisely $w'^2$, in constitutive equation for the computation of normal stress we obtain

$$\begin{aligned}
&\int_0^{L_e} \Big[EA.(\sum_{i=1}^{n=2}\sum_{j=1}^{n=2} N'_i.N'_j.\delta u_j.u_i)\Big]\frac{L_e}{2}d\xi_1 + \\
&\int_0^{L_e} \Big[EI.(\sum_{I=1}^{m=4}\sum_{J=1}^{m=4} H''_I.H''_J.\Omega_I.\delta\Omega_J)\Big]\frac{L_e}{2}d\xi_1 + \\
&\int_0^{L_e} \Big[\underbrace{EA.(u' + \frac{1}{2}\underbrace{w'^2}_{0})}_{N}.(\sum_{I=1}^{m=4}\sum_{J=1}^{m=4} H'_I.H'_J.\Omega_I.\delta\Omega_J)\Big]\frac{L_e}{2}d\xi_1
\end{aligned} \tag{5.7}$$

It can be realized that $i, j = (1, 2)$ and $I, J = (1, 2, 3, 4)$, therefore it can also be written in matrix

$$\begin{aligned}
&\begin{bmatrix}\delta u_1 & \delta u_2\end{bmatrix} \underbrace{\int_0^{L_e} EA \begin{bmatrix} N'_1N'_1 & N'_1N'_2 \\ N'_2N'_1 & N'_2N'_2 \end{bmatrix} \frac{L_e}{2}d\xi_1}_{\boldsymbol{k}^{11}} \begin{bmatrix} u_1 \\ u_2 \end{bmatrix} + \\
&\begin{bmatrix}\delta\Omega_1 & \delta\Omega_2 & \delta\Omega_3 & \delta\Omega_4\end{bmatrix} \underbrace{\int_0^{L_e} EI \begin{bmatrix} H''_1H''_1 & H''_1H''_2 & H''_1H''_3 & H''_1H''_4 \\ H''_2H''_1 & H''_2H''_2 & H''_2H''_3 & H''_2H''_4 \\ H''_3H''_1 & H''_3H''_2 & H''_3H''_3 & H''_3H''_4 \\ H''_4H''_1 & H''_4H''_2 & H''_4H''_3 & H''_4H''_4 \end{bmatrix} \frac{L_e}{2}d\xi_1}_{\boldsymbol{k}^{22^{(1)}}} \begin{bmatrix} \Omega_1 \\ \Omega_2 \\ \Omega_3 \\ \Omega_4 \end{bmatrix} + \\
&\begin{bmatrix}\delta\Omega_1 & \delta\Omega_2 & \delta\Omega_3 & \delta\Omega_4\end{bmatrix} \underbrace{\int_0^{L_e} EA.u'_e \begin{bmatrix} H'_1H'_1 & H'_1H'_2 & H'_1H'_3 & H'_1H'_4 \\ H'_2H'_1 & H'_2H'_2 & H'_2H'_3 & H'_2H'_4 \\ H'_3H'_1 & H'_3H'_2 & H'_3H'_3 & H'_3H'_4 \\ H'_4H'_1 & H'_4H'_2 & H'_4H'_3 & H'_4H'_4 \end{bmatrix} \frac{L_e}{2}d\xi_1}_{\boldsymbol{k}^{22^{(2)}}} \begin{bmatrix} \Omega_1 \\ \Omega_2 \\ \Omega_3 \\ \Omega_4 \end{bmatrix}
\end{aligned} \tag{5.8}$$

The stiffness matrix of one element for beam based on Second Order theory $\boldsymbol{k}^{II}$ can be expressed

$$\begin{bmatrix} \delta\boldsymbol{u}_i & \delta\boldsymbol{\Omega}_I \end{bmatrix} \underbrace{\left[\begin{array}{c|c} \boldsymbol{k}^{11} & \boldsymbol{0} \\ \hline \boldsymbol{0} & \boldsymbol{k}^{22^{(1)}} + \boldsymbol{k}^{22^{(2)}} \end{array}\right]}_{\boldsymbol{k}^{II}} \underbrace{\begin{bmatrix} \boldsymbol{u}_i \\ \boldsymbol{\Omega}_I \end{bmatrix}}_{\boldsymbol{\Lambda}} = \begin{bmatrix} \delta\boldsymbol{u}_i & \delta\boldsymbol{\Omega}_I \end{bmatrix} \begin{bmatrix} \boldsymbol{F}^1 \\ \boldsymbol{F}^2 \end{bmatrix} \quad \text{with}$$

$$k_{II} = \left[\begin{array}{c|c|c|c|c|c} k^{11}_{11} & k^{11}_{12} & 0 & 0 & 0 & 0 \\ \hdashline k^{11}_{21} & k^{11}_{22} & 0 & 0 & 0 & 0 \\ \hdashline 0 & 0 & k^{22^{(1)}}_{11} + k^{22^{(2)}}_{11} & k^{22^{(1)}}_{12} + k^{22^{(2)}}_{12} & k^{22^{(1)}}_{13} + k^{22^{(2)}}_{13} & k^{22^{(1)}}_{14} + k^{22^{(2)}}_{14} \\ \hdashline 0 & 0 & k^{22^{(1)}}_{21} + k^{22^{(2)}}_{21} & k^{22^{(1)}}_{22} + k^{22^{(2)}}_{22} & k^{22^{(1)}}_{23} + k^{22^{(2)}}_{23} & k^{22^{(1)}}_{24} + k^{22^{(2)}}_{24} \\ \hdashline 0 & 0 & k^{22^{(1)}}_{31} + k^{22^{(2)}}_{31} & k^{22^{(1)}}_{32} + k^{22^{(2)}}_{32} & k^{22^{(1)}}_{33} + k^{22^{(2)}}_{33} & k^{22^{(1)}}_{34} + k^{22^{(2)}}_{34} \\ \hdashline 0 & 0 & k^{22^{(1)}}_{41} + k^{22^{(2)}}_{41} & k^{22^{(1)}}_{42} + k^{22^{(2)}}_{42} & k^{22^{(1)}}_{43} + k^{22^{(2)}}_{43} & k^{22^{(1)}}_{44} + k^{22^{(2)}}_{44} \end{array}\right], \begin{bmatrix} \boldsymbol{u}_i \\ \boldsymbol{\Omega}_I \end{bmatrix} = \begin{bmatrix} u_1 \\ u_2 \\ \Omega_1 \\ \Omega_2 \\ \Omega_3 \\ \Omega_4 \end{bmatrix} \tag{5.9}$$

## 5.4 Discretization of the Linearization of the Weak Form

The complete linearization of weak form (5.5) can be derived with constitutive equation in equation (5.4). we obtain

$$DG(u, w, \delta u, \delta w).\Delta\boldsymbol{\Lambda} = \int_0^l (\delta\epsilon.EA.\Delta\epsilon + \delta\kappa.EI.\Delta\kappa)dX_1 + \int_0^l (\Delta\delta\epsilon.N + \Delta\delta\kappa.M)dX_1 \tag{5.10}$$

The parameters $\delta\epsilon$, $\delta\kappa$, $\Delta\epsilon$, $\Delta\kappa$, $N$, $M$, $\Delta\delta\epsilon$ and $\Delta\delta\kappa$ are described in equations $(5.2)^1$, $(5.2)^3$, $(4.19)^1$, $(4.19)^2$, $(5.4)^1$, $(5.4)^2$, $(4.22)^1$ and $(4.22)^2$ respectively.Then the above equation for one element could be written

$$\int_0^{L_e} \delta u'_e.EA.\Delta u'_e dX_1 + \int_0^l \delta w''_e.EI.\Delta w''_e dX_1 + \int_0^{L_e} \delta w'_e.\Delta w'_e.N_e dX_1 \tag{5.11}$$

By inserting equations (4.11) to above formulation we obtain

$$\begin{aligned} &\int_0^{L_e} \Big[EA.(\sum_{i=1}^{n=2}\sum_{j=1}^{n=2} N'_i.N'_j.\delta u_j.\Delta u_i)\Big]\frac{L_e}{2}d\xi_1 + \\ &\int_0^{L_e} \Big[EI.(\sum_{I=1}^{m=4}\sum_{J=1}^{m=4} H''_I.H''_J.\Delta\Omega_I.\delta\Omega_J)\Big]\frac{L_e}{2}d\xi_1 + \\ &\int_0^{L_e} \Big[\underbrace{EA.(u' + \frac{1}{2}\underbrace{w'^2}_{0})}_{N}.(\sum_{I=1}^{m=4}\sum_{J=1}^{m=4} H'_I.H'_J.\Delta\Omega_I.\delta\Omega_J)\Big]\frac{L_e}{2}d\xi_1 \end{aligned} \tag{5.12}$$

It can be realized that $i, j = (1, 2)$ and $I, J = (1, 2, 3, 4)$, therefore it can also be written in matrix

$$
\begin{bmatrix} \delta u_1 & \delta u_2 \end{bmatrix} \underbrace{\int_0^{L_e} EA \begin{bmatrix} N_1'N_1' & N_1'N_2' \\ N_2'N_1' & N_2'N_2' \end{bmatrix} \frac{L_e}{2} d\xi_1}_{\boldsymbol{t}^{11} = \boldsymbol{k}^{11}} \begin{bmatrix} \Delta u_1 \\ \Delta u_2 \end{bmatrix} +
$$

$$
\begin{bmatrix} \delta\Omega_1 & \delta\Omega_2 & \delta\Omega_3 & \delta\Omega_4 \end{bmatrix} \underbrace{\int_0^{L_e} EI \begin{bmatrix} H_1''H_1'' & H_1''H_2'' & H_1''H_3'' & H_1''H_4'' \\ H_2''H_1'' & H_2''H_2'' & H_2''H_3'' & H_2''H_4'' \\ H_3''H_1'' & H_3''H_2'' & H_3''H_3'' & H_3''H_4'' \\ H_4''H_1'' & H_4''H_2'' & H_4''H_3'' & H_4''H_4'' \end{bmatrix} \frac{L_e}{2} d\xi_1}_{\boldsymbol{t}^{22^{(1)}} = \boldsymbol{k}^{22^{(1)}}} \begin{bmatrix} \Delta\Omega_1 \\ \Delta\Omega_2 \\ \Delta\Omega_3 \\ \Delta\Omega_4 \end{bmatrix} +
$$

$$
\begin{bmatrix} \delta\Omega_1 & \delta\Omega_2 & \delta\Omega_3 & \delta\Omega_4 \end{bmatrix} \underbrace{\int_0^{L_e} EA.u_e' \begin{bmatrix} H_1'H_1' & H_1'H_2' & H_1'H_3' & H_1'H_4' \\ H_2'H_1' & H_2'H_2' & H_2'H_3' & H_2'H_4' \\ H_3'H_1' & H_3'H_2' & H_3'H_3' & H_3'H_4' \\ H_4'H_1' & H_4'H_2' & H_4'H_3' & H_4'H_4' \end{bmatrix} \frac{L_e}{2} d\xi_1}_{\boldsymbol{t}^{22^{(2)}} = \boldsymbol{k}^{22^{(2)}}} \begin{bmatrix} \Delta\Omega_1 \\ \Delta\Omega_2 \\ \Delta\Omega_3 \\ \Delta\Omega_4 \end{bmatrix}
\tag{5.13}
$$

The tangent stiffness matrix of one element for beam based on Bernoulli theory $\boldsymbol{t}^{II}$ can be expressed

$$
\begin{bmatrix} \delta\boldsymbol{u}_i & \delta\boldsymbol{\Omega}_I \end{bmatrix} \underbrace{\left[\begin{array}{c|c} \boldsymbol{t}^{11} & 0 \\ \hline 0 & \boldsymbol{t}^{22^{(1)}} + \boldsymbol{t}^{22^{(2)}} \end{array}\right]}_{\boldsymbol{t}^{II}} \underbrace{\begin{bmatrix} \Delta\boldsymbol{u}_i \\ \Delta\boldsymbol{\Omega}_I \end{bmatrix}}_{\Delta\boldsymbol{\Lambda}}
\tag{5.14}
$$

with

$$
\boldsymbol{t}^{II} = \left[\begin{array}{c|c|c|c|c|c}
t_{11}^{11} & t_{12}^{11} & 0 & 0 & 0 & 0 \\ \hline
t_{21}^{11} & t_{22}^{11} & 0 & 0 & 0 & 0 \\ \hline
0 & 0 & t_{11}^{22^{(1)}} + t_{11}^{22^{(2)}} & t_{12}^{22^{(1)}} + t_{12}^{22^{(2)}} & t_{13}^{22^{(1)}} + t_{13}^{22^{(2)}} & t_{14}^{22^{(1)}} + t_{14}^{22^{(2)}} \\ \hline
0 & 0 & t_{21}^{22^{(1)}} + t_{21}^{22^{(2)}} & t_{22}^{22^{(1)}} + t_{22}^{22^{(2)}} & t_{23}^{22^{(1)}} + t_{23}^{22^{(2)}} & t_{24}^{22^{(1)}} + t_{24}^{22^{(2)}} \\ \hline
0 & 0 & t_{31}^{22^{(1)}} + t_{31}^{22^{(2)}} & t_{32}^{22^{(1)}} + t_{32}^{22^{(2)}} & t_{33}^{22^{(1)}} + t_{33}^{22^{(2)}} & t_{34}^{22^{(1)}} + t_{34}^{22^{(2)}} \\ \hline
0 & 0 & t_{41}^{22^{(1)}} + t_{41}^{22^{(2)}} & t_{42}^{22^{(1)}} + t_{42}^{22^{(2)}} & t_{43}^{22^{(1)}} + t_{43}^{22^{(2)}} & t_{44}^{22^{(1)}} + t_{44}^{22^{(2)}}
\end{array}\right]
\tag{5.15}
$$

It has to be considered that for integration matrix $t^{22^{(2)}}$ one-point Gauss quadrature should be evaluated and for all other coefficient two-point quadrature.

# Chapter 6

# Example Results

In this chapter the results of three examples will be expressed and the difference between the four Beam Theories will be expressed.

## 6.1 Lee's Frame

Lee's frame is loaded by a point load at location shown in Figure (6.1) in vertical direction. The beam and column have the same material data. $EA = 10^6$, $EI = 2.10^5$ and $G\hat{A} = 10^5$. Twenty finite beam element are applied to discretize the structure.

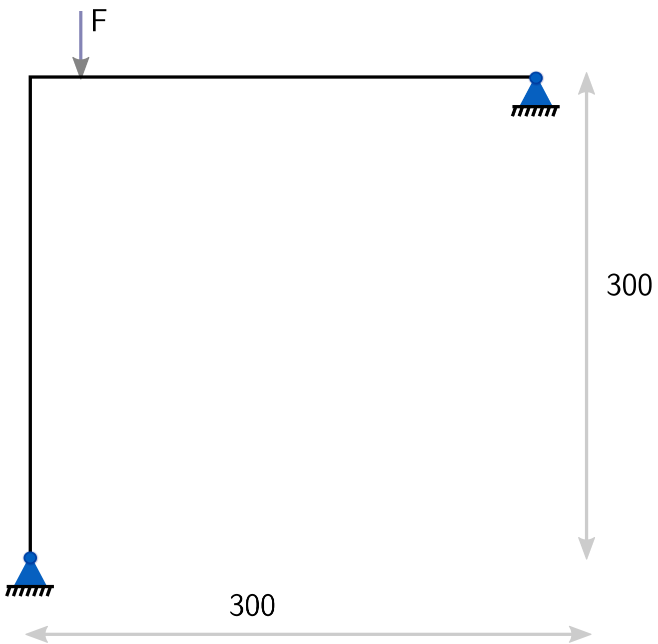


*Figure 6.1: Lee's Frame*

Figure (6.2) shows deformed configuration for a load factor $\lambda = 45$, which was computed with geometrically exact beam model. (See Chapter 2). Figure (6.3) depicts the load-deflection curves for geometrically exact model, the theory of moderate rotation, the Bernoulli beam

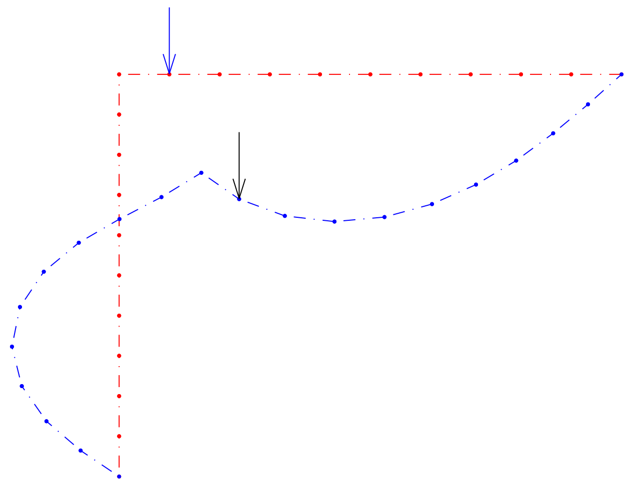

*Figure 6.2: Deformed structure for load factor $\lambda = 45$*

theory and second order beam theory. The computation of load-deflection curve is performed by using an arc-length method and to optimize the process time the adaptive length have been implemented. In this plot the load is plotted versus the vertical displacement under the point load. Differences are clearly visible. The classical second order theory follows the results of the geometrically exact theory only for small displacements and hence can only be applied for problems with small displacements and rotations. Hence the second order theory cannot be applied to model post-critical states of structures. However, since many beam structures only

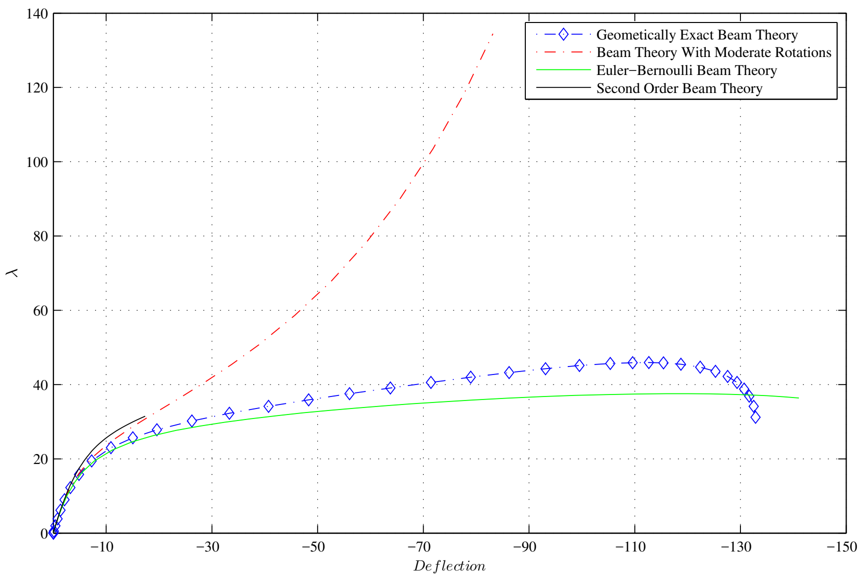


*Figure 6.3: Load-Deflection curve of Lee's Frame*

undergo small displacements and rotations in practical applications, the second order theory has its eligibility.
The theory of moderate rotations based on chapter 3 is closer to the exact model, but deviates from the result of the geometrically exact theory when the load factor is larger than $\lambda = 28$. It is interesting to note that Bernoulli beam theory recovers the correct tendency of the solution and hence can be used to estimate the behavior in post-critical states.
For geometrically exact beam model, the frame also analyzed with different polynomial grade for shape functions. As it can be clearly seen in Figure (6.4), there is a small difference in convergence between $P = 1$ and other polynomial grades. Although the results gained from

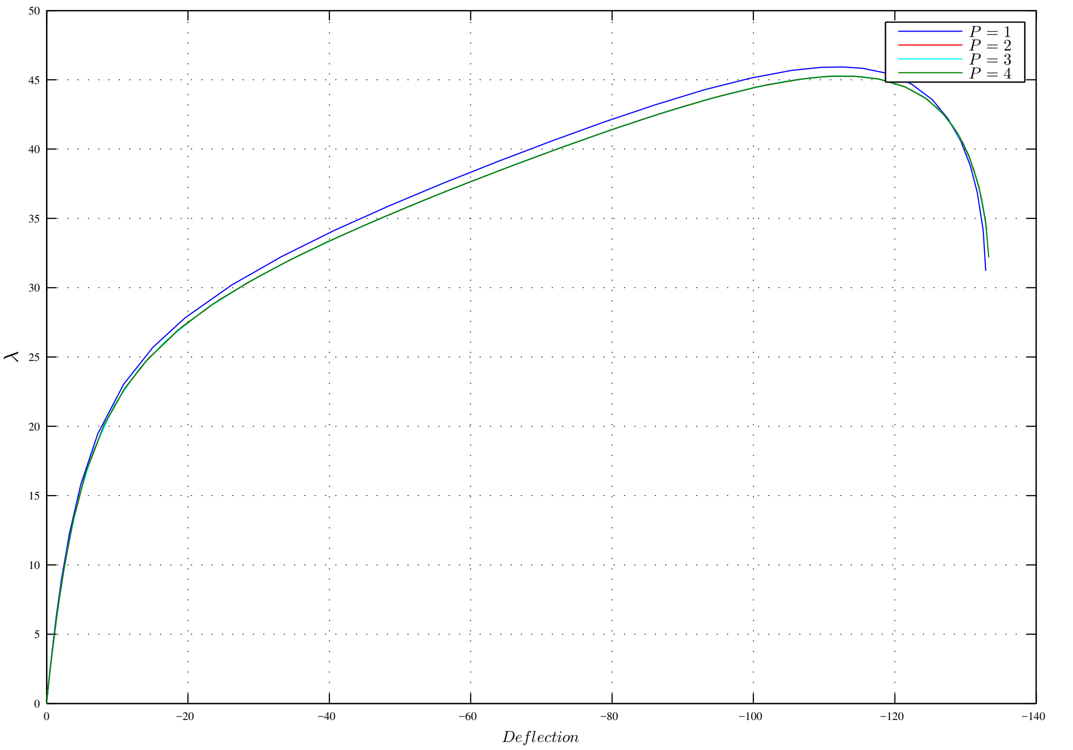


*Figure 6.4: Load-Deflection curve of Lee's Frame with Different Polynomial Grade*

higher order polynomial is more accurate but the time of process is without doubt longer and the difference between results in $P = 1$ and $P = 2$ is about $1.9\%$ which this amount of deviation quiet acceptable. Thus in many cases of analysis of exact beam model to save the the process time, the shape function with $P = 1$ is being implemented.
In Figure (6.5) it can be seen the different configuration of structure under three displacement configurations. The red line is undeformed shape, the blue line is deformed shape with vertical displacement under the point load $= -80$, the green line with vertical displacement under the point load $= -132$ and the black line with vertical displacement under the point load $= -133$. As it can easily been seen, the difference between forth and third configuration is huge, although the displacement is small. Here there is snap-back response in Load-Deflection curve in Figure (6.6). The snap-back response is an exaggerated snap-through, in which the response curve turns back in itself with the consequent appearance of turning points. The equilibrium between the two turning points may be stable and consequently physically realizable. And for definition of Snap-through it can be said that since the tangent at a limit point is normal to $\lambda$, it must

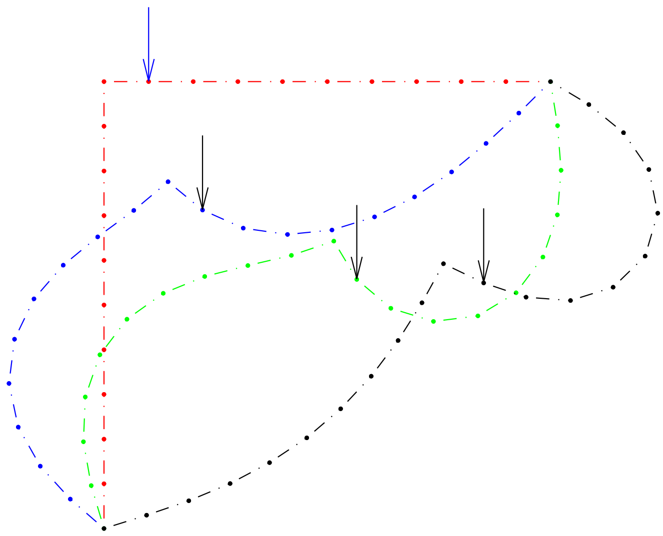

Figure 6.5: Deformed Shape of Structure under Three Different Load

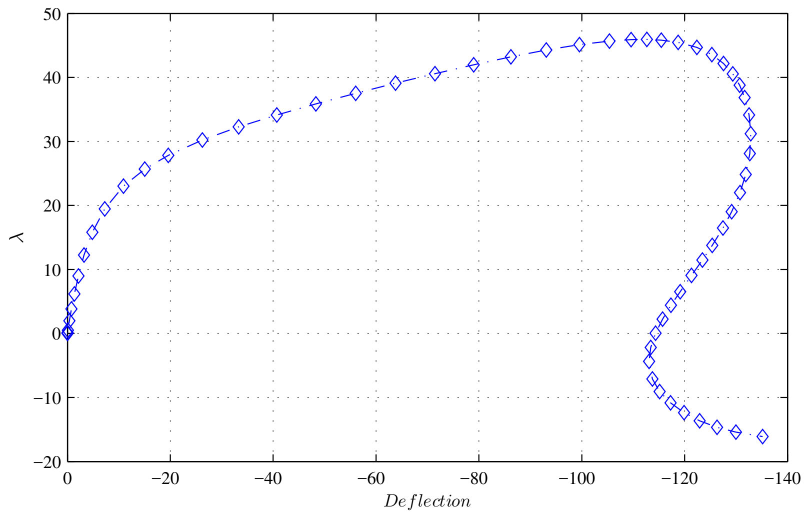


Figure 6.6: Snap-Back Response

correspond to a maximum, minimum orinflexion point with respect to $\lambda$. In the case of a maximum or a minimum, the occurrence of a limit point is informally called snap-through or snap-buckling by structural engineers.

## 6.2 William's Toggle Frame

A frame in Figure (6.7) was first solved analytically and experimentally by F.W Williams. It is sufficient to consider only half of the frame since the problem is symmetric. The problem is considered as a good benchmark for testing non-linear beam elements. The toggle frame is loaded by a point load at the location shown in Figure (6.7). The beams have cross-sectional area of $A = 0.408282\ cm^2$, shear cross section of $\hat{A} = \frac{5}{6}.A = 0.3402\ cm^2$, moment of inertia of $I = 0.0132651\ cm^4$, linear elastic modulus equal to $E = 19971.4\ kN/cm^2$, poisson ratio of $\nu = 0.27$ and shear modulus equal to $G = \frac{E}{2.(1+\nu)} = 7862.75\ kN/cm^2$.
In Figure (6.8) the initial frame configuration and deformed configuration is shown. The two

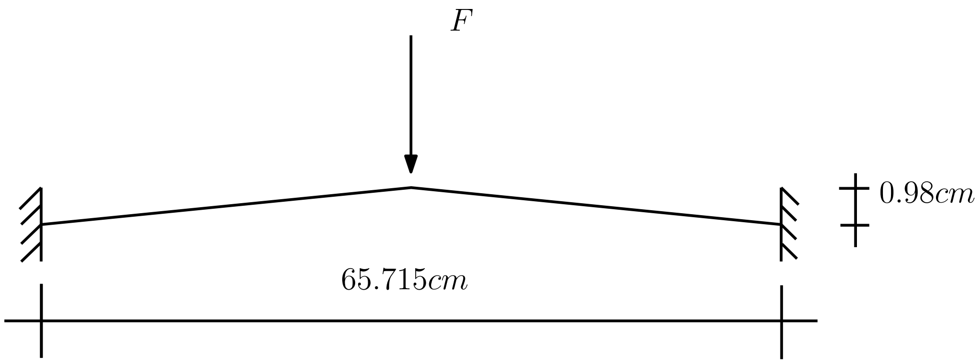


*Figure 6.7: William's Toggle Frame*

beams are discretized with 8 equal length beam elements. This discretization is sufficiently fine so that the load displacement results of Figure (6.9) converge. The displacement plotted against load is the vertical displacement of the node under the point load.

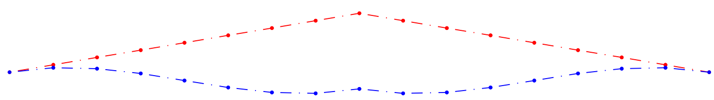

*Figure 6.8: Deformed Configuration*

As far as it can be seen in Figure(6.9), the frame is analyzed with all four beam model. Surprisingly the results between geometrically beam model and moderate rotation can hardly be differentiated. Again the Bernoulli beam result can overlap the geometrically exact beam with a near approximation, but Second order model deviate from geometrically exact model when the load factor is larger than $\lambda = 80$.

## 6.3 Cantilever Beam with Tip Load

In this section a cantilever beam analyzed. This cantilever beam is loaded by a point load at its free end. The initial and final configuration of the beam is shown in Figure (6.10).
The load displacement is linear for small loads, but as the load increases the curve is clearly

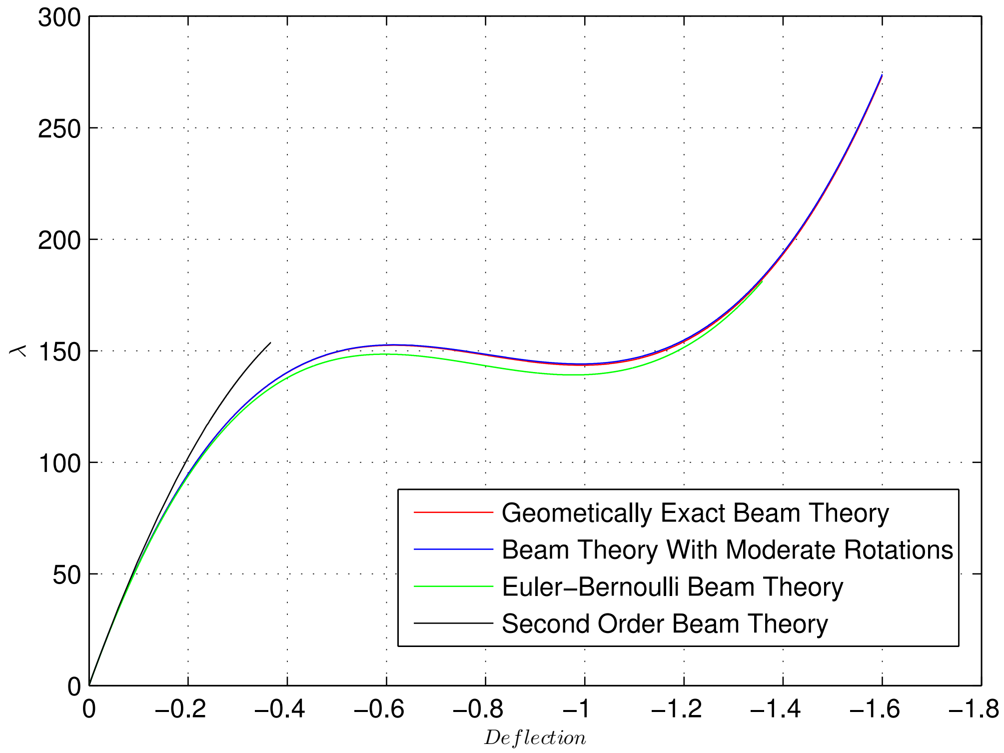


*Figure 6.9: Load-Deflection Curve of Toggle Frame*

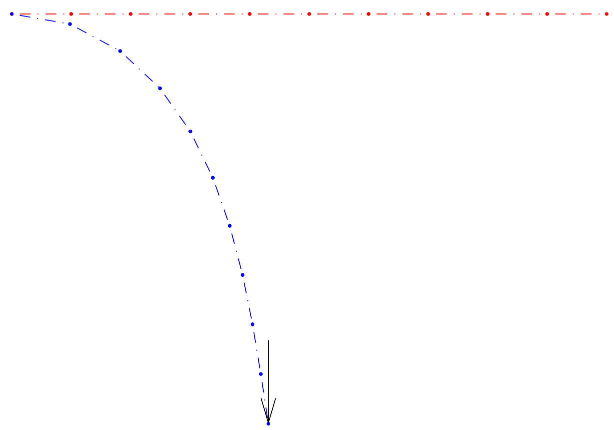

*Figure 6.10: Deformed Configuration of Cantilever Beam*

nonlinear (6.11). As the load increases further the structure becomes stiffer, which is caused by tension stiffening of the beam in its deformed configuration. For this example, all the material data is exactly chosen like Lee's frame. The beam is $300$ long and is discretized with $10$ equal-length beam elements and $11$ nodes.

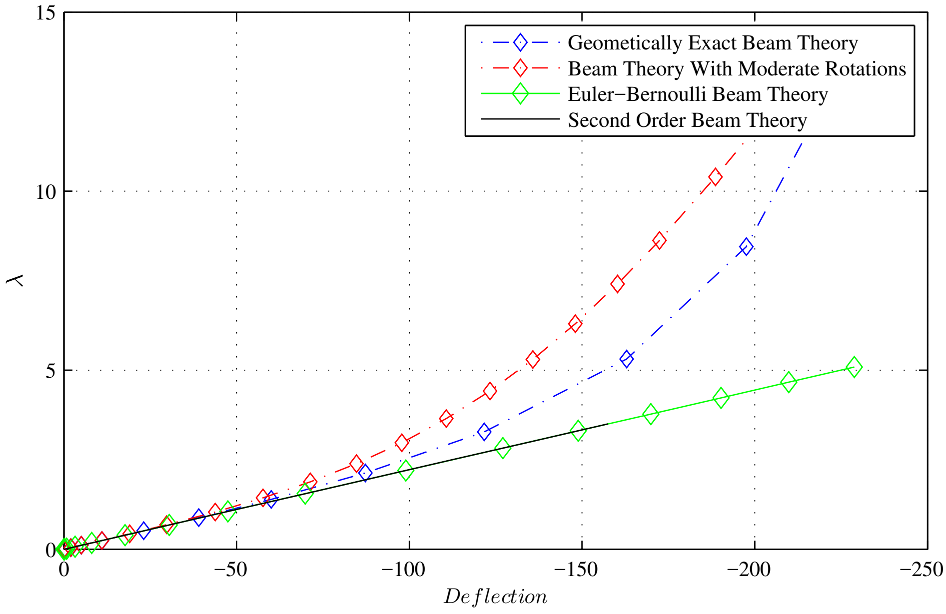


*Figure 6.11: Load-Deflection of Cantilever Beam*

## 6.4 Summary

This section presented a short overview with respect to different beam theories spanning the arc from geometrically exact models to second order theories. For all theoretical models, weak forms were developed and the discretization leading to residuals and tangent matrices for the nonlinear beam theories were derived. In summary, the following statements can be made:

- The effort for the computation of residuals vectors and tangent matrices is almost identical for the geometrically exact model and the approximate theories.
- One can always use the best (geometrically exact) model to discretize beam structures. Such approach ensures that, from the model point of view, the finite element analysis will converge to the correct theoretical solution.
- Exact analytical solution of approximate theories (these can be developed for the second order theory) are not exact when it comes to modelling a nonlinear beam problem.
- From the results of the example in Figures (6.1) and (6.7), it can be deduced that approximate theories are useful for a wide range of problems in which the effects of the nonlinear behavior yield only small displacements and rotations.